Hubless E-bike Design Project

Final Report

Isaac Einstein

Connor Halford

Amanda Weiskind

Avery Zwayer

Executive Summary

The goal of this project was to create a hubless E-bike drivetrain utilizing both an electric motor and traditional human power. To begin, the team first conducted industry research and decided on an overall factor of safety of 2.52. Then, the DC motor capability was compared to the desired performance of other bicycles and riders. The critical load for the drivetrain was determined to be 300 lbs. loaded onto the pedal, representing a rider pedaling with their full body weight. It was established that the motor should operate at 3000 rpm and the bicycle should have a top speed of 13 mph; this resulted in an overall velocity ratio of 0.0502. Also, it was determined that a cadence of 80 rpm from the crank was most comfortable and efficient for the rider.

Torque transfer elements were then mapped and sourced to accomplish the performance and spatial constraints. The simplest layout consisted of nine spur gears, one internal gear, two sprockets, and one chain. The required torque, strength, teeth, and radius or length of each component were incrementally analyzed and then used to source purchasable components. Once viable components were decided, the resultant forces were found.

The resultant forces were used to find axial and radial load requirements for the shafts and bearings. Following a similar process as before, multiple shafts were chosen on certain diameters and strengths. Based on the team's research, the desired life of the bearings was determined to be 12,000 hours. Purchasable bearings were analyzed and determined with catalog ratings and the bearing life equations. Throughout this process, all components were ensured to have compatible sizes.

A solution for the rear wheel support bearings was then devised. After analyzing all applicable forces on the rear wheel assembly, it was determined that the Misumi needle cam

follower bearings spaced 120° apart were viable solutions. The final assembly model for the rear wheel and drivetrain is shown in Figure 1, and close-up visuals of different components are found later in their respective design chapters.

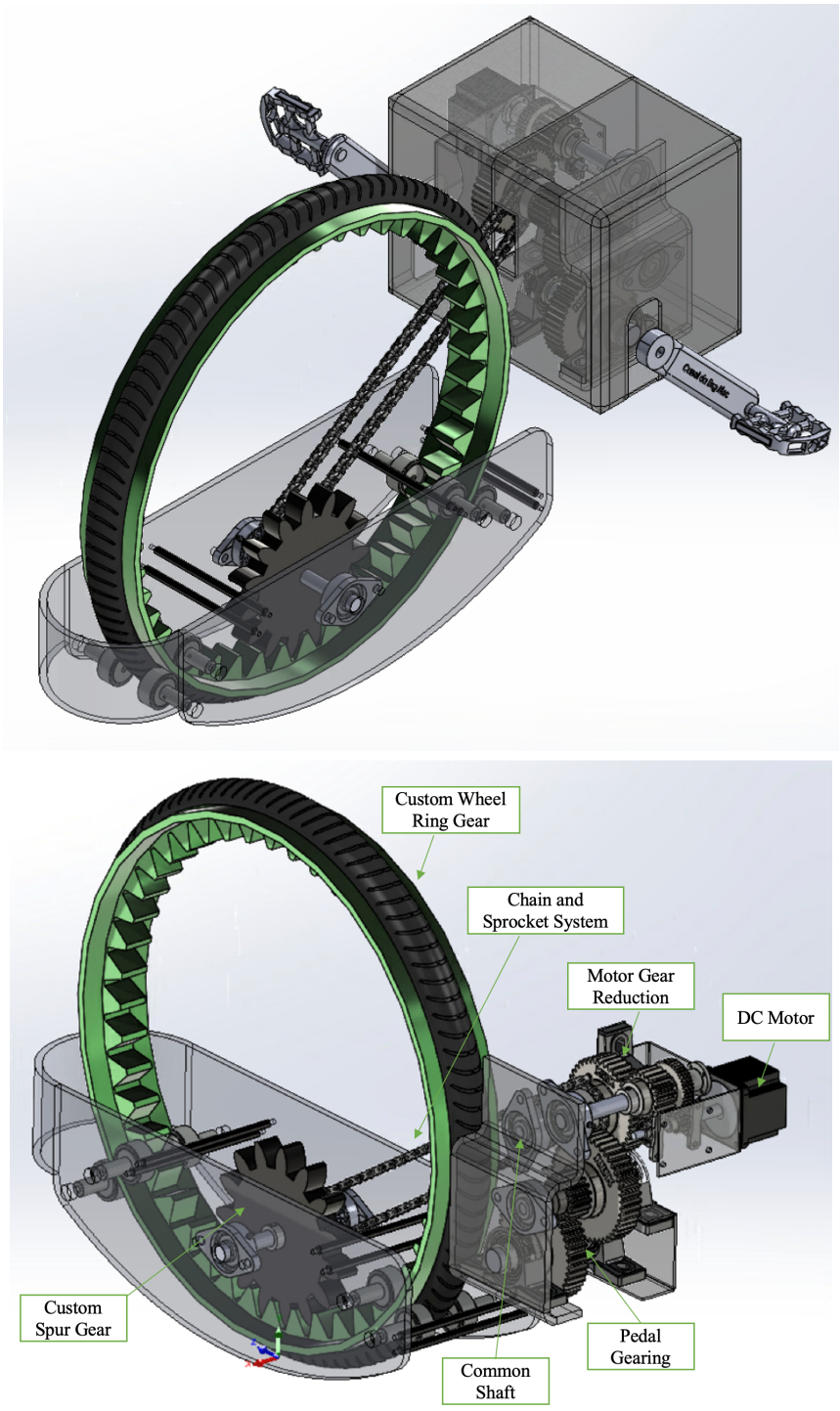

Figure 1: Full Assembly

Table of Contents

List of Figures

List of Tables

Chapter 1: FOS and VR

Factor of Safety

The Factor of Safety (FOS) is the ratio of a component's ultimate stress to the working stress (8). The FOS value – always greater than 1 for a safe design – ensures that there is a buffer between applied stress and a design's proximity to yielding in case calculated strength or applied load simulations are not reliable. Choosing a desired FOS value involves determining the reliability of materials, the reliability of the component in the context of an assembly, and the ease of manufacturing. Many materials and applications have standard FOS values, which can be used or logically expanded upon for new designs.

There are many factors that may increase or decrease the required FOS depending on the user's intended needs for this machine. Some use cases that may conservatively increase the necessary FOS are possible collisions, jumping, and other tricks or skills. Studies show that mountain bikers are at an elevated risk of injury compared to on-road bikers (18). Thus, there is likely a need for increased FOS to better protect against rider injuries. Additionally, mountain bikes likely need a higher FOS to withstand the heavy force from tricks such as jumps.

The critical load for the drivetrain stems from the weight of the rider. A rider putting all their body weight onto a pedal would correlate to the maximum force experienced by the drivetrain. Most bicycles are designed for riders up to 300 lbs (4). Therefore, the critical load for the drivetrain is 300 lbf pushing down on the face of the pedal.

Before calculating the necessary FOS of the drivetrain, a reference FOS of the bike frame was researched. One study using FEM to evaluate five load cases on a mountain bike frame during each load case determined the minimum FOS for each stage (15). These different factors of safety are shown in Table 1 below.

Table 1: FOS for Mountain Bike Frame for Each Load Case

Alloys	Factor of Safety Obtained For Different Cases				
	Static Start Up	Steady State Pedaling	Vertical Impact	Horizontal Impact	Rear Wheel Braking
Aluminum 6061-T	11.87	11.62	5.93	9.52	15
Aluminum 7005-T	15	15	14.5	9.77	15

The limiting FOS across all load cases was 5.93 during vertical impact. When using reliable materials in a severe environment, it is recommended to use a FOS of 3 or greater (24). This FOS of 5.93 is still above the safe design FOS of 3, meaning under each load case common bike frame alloys will withstand necessary stresses without failing (15).

One report analyzed the stress found in a drivetrain while biking, specifically the pedal axle and crank as these components were determined to experience the most stress (3). This analysis was done with aluminum 2014 which has a yield strength of 414 MPa. The maximum stress found in the pedal axle and crank were 164 MPa for each component. Using the provided yield strength, the drivetrain is experiencing a FOS of 2.52. This can be seen in Equation 1 below.

$$Factor\ of\ Safety = \frac{Yield\ Strength}{Experienced\ Stress} = \frac{414\ MPa}{164\ MPa} = 2.52 \quad (1)$$

The drivetrain will be built from reliable materials and should not undergo extreme conditions. As a result, the recommended FOS is 2 or greater (24). Therefore, the drivetrain is built safely with a FOS of 2.52.

One report on the structural analysis of a bicycle drivetrain found that "through structural analysis and pedal load analysis, the drivetrain was confirmed to have a very low risk of structural failure" (12). This confirms the difference of FOS between the frame (5.93) and the drivetrain (2.52) which implies that the frame is more likely to fail and thus requires a larger safety tolerance. Because the drivetrain is unlikely to fail, it is safe to assume that the FOS--found above--of 2.52 can be used without any additional tolerances.

As a result, the recommended FOS for the drivetrain for this project is 2.52.

Overall Drivetrain Velocity Ratio

The drivetrain Velocity Ratio (VR) is the ratio of the system's output speed over the input speed, as specified in Equation 2. A higher VR implies a lower torque ratio, and a lower VR implies a higher torque ratio.

$$VR = \frac{output\ speed}{input\ speed} = \frac{Desired\ Top\ Speed}{Motor\ Output\ Speed} \tag{2}$$

Given that this hubless electric bicycle is designed to be a mountain bike traveling through rougher terrain, a higher torque will be desired compared to that of an urban commuter bicycle.

When selecting a wheel diameter, the ISO standard tire dimensions were considered against the purpose of the design. The most common wheel diameters for mountain applications include the 27.5" and 29" dimensions (8). In addition to this, the desired top speed for the bike was determined to be 13 MPH to maintain similar performance to current electric mountain bikes (29). Considering both wheel diameter options, the speed in revolutions per minute (RPM) of both wheels given the desired speed of 13 MPH, was calculated using Equation 3 and is listed in Table 2 below.

$$Speed(RPM) = \frac{Speed(MPH)}{60} * \frac{63360}{\pi Dwheel} \quad (3)$$

Table 2: Speed Comparison of 27.5” and 29” Wheel Diameters.

Wheel Diameter (in)	**27.5**	**29**
Speed (RPM)	159	151

A 350W brushless DC motor with a wide speed range was selected for the bicycle. The motor specifications and speed-torque curve for this motor were consulted to determine motor speed options with the corresponding motor torque output produced based on the rated operating torque line, as shown in Figure 2 below.

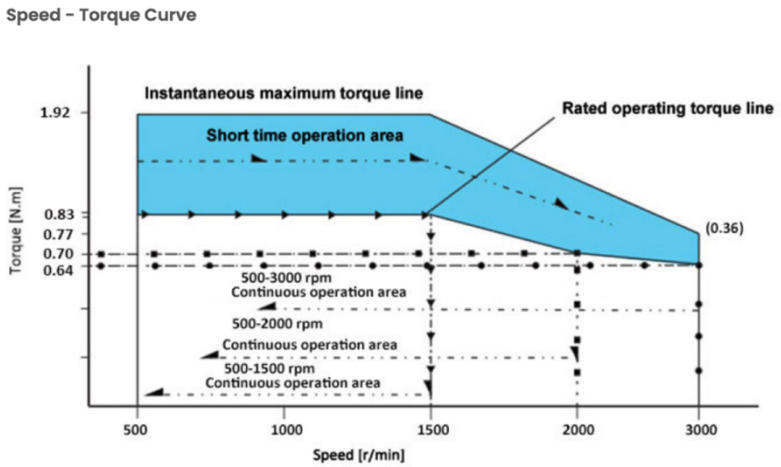

Figure 2: Speed-Torque Curve for the 350W Brushless DC Motor.

The rated operating torque line is referenced as the rated torques at this line allow the motor to run for a long time, which is necessary for the planned use of the motor for this electric mountain bicycle. The following three speeds were chosen for further analysis: 1500, 2000, and 3000 rpm. The corresponding torque at these speeds includes 0.83, 0.70, and 0.64 Nm, respectively. Using this data from the curve and the speed comparisons in Table 2, the

mechanical output power, efficiency, and velocity ratios could be calculated using Equations 4, 5, and 2, respectively.

$$Power_{Output} = \omega \cdot T = speed \cdot \frac{2\pi}{60} \cdot T\ [W] \quad (4)$$

$$\eta = \frac{P_{output}}{P_{input}} = \frac{P_{output}}{350W} \quad (5)$$

The calculation of these factors is summarized in Table 3 below, with velocity ratios for the 27.5" and 29" wheel diameters and each motor speed, respectively.

Table 3: Output Power, Efficiency, and Velocity Ratios.

Motor Speed (RPM)	**Motor Speed (Rad/s)**	**Motor Torque (Nm)**	**Mechanical Output Power [W]**	**Efficiency**	**VR (27.5 D)**	**VR (29 D)**
1500	157.1	0.83	130.4	0.37	0.1059	0.1005
2000	209.4	0.7	146.6	0.42	0.0795	0.0753
3000	314.2	0.64	201.1	0.57	0.0530	0.0502

This analysis reveals that the motor torque at the three motor speed selections are relatively close in magnitude, with the torque between 1500 and 3000 RPM decreasing by 0.19Nm for double the speed. The mechanical output power, and thus the efficiency, increases as the motor speed increases. Based on this data analysis, the velocity ratios for each wheel diameter are roughly the same at each motor speed. Given the bike application, as mentioned, the desired velocity ratio is one of a lower value to produce higher torque and mechanical power output. Thus, the 3000-rpm motor speed with 0.64 Nm motor torque will be selected due to its high mechanical output power, high efficiency, and low velocity ratios. Since the velocity ratios between the 27.5" and 29" bikes are relatively equal, the bike wheel size selection will be based on the following factors: stability, acceleration, ability to ride on rough terrain, and control. Although the 29" diameter has a slower acceleration due to the slightly larger wheel size, it is

more stable, has greater traction with rough terrain, and it is easy for riders to maintain control and speed (7). Therefore, the velocity ratio of 0.0502 is chosen for the 29” wheel diameter.

Chapter 2: Detailed Design of Torque Transfer Elements

Torque Transfer Element Design

To achieve a total velocity reduction of 20:1 from the motor, spinning at 3000 rpm, to the 29” diameter wheel, spinning at ~151 rpm, a combination of gears and chains was incorporated into the E-bicycle design. Given that each set of gears or chain sprockets can achieve a maximum reduction of 3:1, these components must be compounded to achieve the total necessary reduction.

Since the E-bicycle still operates via a pedal that is motor-assisted, the average speed of rotation of the pedal had to be considered in the design. It was found that a moderate pedaling cadence is between 80-100 rpm (16). For this design, since the bicycle is electronically assisted, the lower limit of this range was considered, given the cadence is likely reduced due to the motor assistance. Thus, a speed increase is needed between the pedaling speed of 80 rpm and the rear wheel output speed of around 151 rpm, whereas a reduction is needed between the motor and wheel. It was decided that both the motor and pedal would have separate gearing that generates an output speed of 500 rpm at a common shaft. Also attached to this common shaft is a sprocket that chains this shaft rotating at 500 rpm to gearing at the wheel. There are six gear reductions or increases within the drivetrain to achieve the desired output speed for the given inputs. Figure 3 shows a rough layout of the pedal gear ratios.

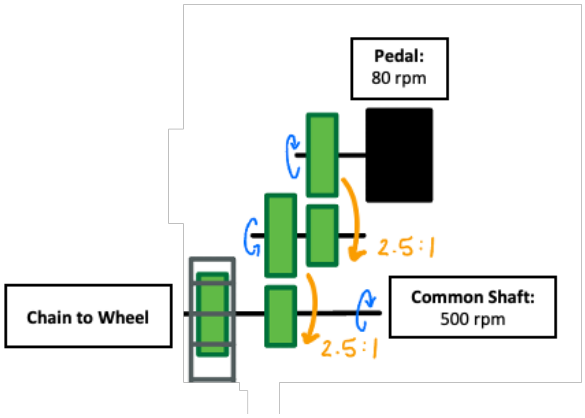

Figure 3: Pedal Gear Assembly

The pedal has a compound gear ratio of 25:4 in total which is achieved by a 2.5:1 gear pairing to connect to the 500-rpm shaft. This is found through Equation 6.

$$\frac{\omega_{shaft}}{\omega_{pedal}} = \frac{500\ rpm}{80\ rpm} = \left(\frac{2.5}{1}\right)\left(\frac{2.5}{1}\right) = \left(\frac{25}{4}\right) \tag{6}$$

Figure 4 depicts the motor gearing. As shown in Figure 1, this will be housed in the center of the bike frame.

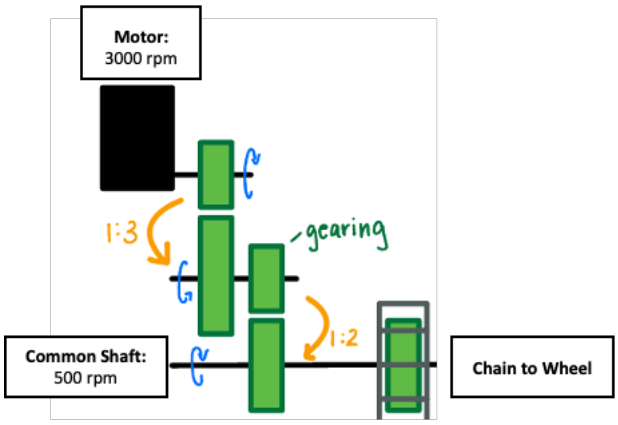

Figure 4: Motor Gear Assembly

As shown in Equation 7, the motor has a compound gear ratio of 1:6 in total which is achieved by two reductions of 1:3 and then 1:2 to connect the motor shaft to the 500-rpm shaft.

$$\frac{\omega_{shaft}}{\omega_{motor}} = \frac{500\ rpm}{3000\ rpm} = \left(\frac{1}{3}\right)\left(\frac{1}{2}\right) = \left(\frac{1}{6}\right) \tag{7}$$

Once the shaft is reached and the pedal and motor have been geared to a common speed, two sprockets are chained together with a small gear reduction of 18:19. The wheel driver gear, that is in direct contact with the wheel teeth, is mounted to the same shaft as the rear chain sprocket. To achieve the final necessary speed reduction, there is a gear ratio of 1:3 between the driver gear and the driven wheel. Thus, with this gearing system, the output speed of the wheel is 157 rpm (Equation 8).

$$\frac{\omega_{wheel}}{\omega_{shaft}} = \frac{157.8\ rpm}{500\ rpm} = \left(\frac{18}{19}\right)\left(\frac{1}{3}\right) = \left(\frac{6}{19}\right) \tag{8}$$

The design consists of 9 gears, 2 sprockets, 1 chain, and 1 wheel with internal teeth in total. The complete layout of all components is shown below in Figure 5.

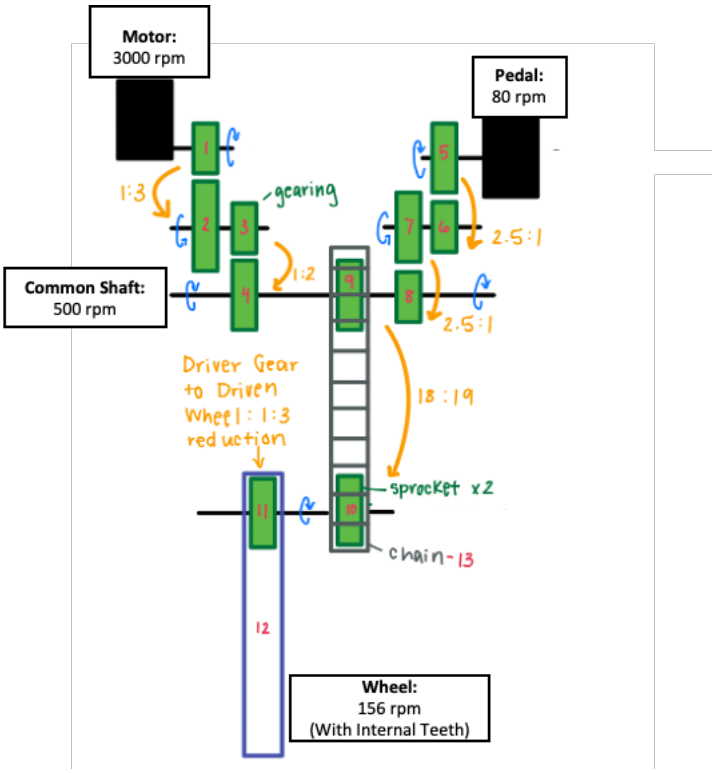

Figure 5: Full Gearing Assembly

Each of the gears that make up the drivetrain will be spur gears given that they are less expensive and easier to manufacture than helical gears. They also are highly efficient in power transmission which is important to minimize energy loss during pedaling. A chain was incorporated for transmitting torque across a larger distance from the common shaft to near the rear wheel. Eight spur gears, two sprockets, and one chain will be selected from catalogs following torque, force, and strength analysis. Two custom spur gears will also be designed for the driver and driven internal wheel gears, components 11 and 12, to make up the final 1:3 reduction in Figure 5 above.

Torque Analysis of Components

To calculate the forces in each of the drivetrain components, the torque in each element is first calculated using Equation 9 below.

$$T_{out} = \frac{1}{VR} * T_{in} \tag{9}$$

The known torque output of the motor at 3000 rpm is 0.64 Nm as listed on the torque-speed curve. To calculate the torque output at the pedal, the weight of the biker and the crank length of the pedal is needed. To achieve a conservative design, it is assumed that the biker is at the maximum weight limit of mountain bicycles and is standing up, applying full force to the pedal. Research provided that the maximum weight limit of a human riding a mountain bicycle is typically 300 lb or 1335 N and the typical crank length is 175 mm or 0.175 m (14). Thus, the torque output at the pedal can be calculated using Equation 10 below. The torque from the pedal is 233.63 Nm.

$$T_{pedal} = F_{human} * l_{crank} \tag{10}$$

Table 4 includes the torque in each component calculated using Equation 10.

Table 4: Torque in Each Drivetrain Component.

No.	1	2	3	4	5	6	7	8	9	10	11	12
Torque (Nm)	0.64	1.92	1.92	3.84	233.6	93.5	93.5	37.4	41.2	43.5	43.5	130.5

The torque output at the wheel is calculated to be 130.5 Nm. The full analysis can be seen below.

Motor Torque: $T_m = 0.64\ Nm$

$T_1 = T_m = 0.64\ Nm \rightarrow T_2 = \frac{1}{1/3} T_1 = 1.92\ Nm$ $\quad$ $T_3 = T_2 = 1.92\ Nm \rightarrow T_4 = \frac{1}{1/2} T_3 = 3.84\ Nm$

Assume: Human: $300\ lb = 1335\ N$ $\quad$ Crank Length: $175mm = 0.175m$

Pedal Torque: $T_p = 1335(0.175) = 233.63\ Nm$

$T_5 = T_p = 233.63\ Nm \rightarrow T_6 = \frac{1}{2.5/1} T_5 = 93.45\ Nm$

$T_7 = T_6 = 93.45\ Nm \rightarrow T_8 = \frac{1}{2.5/1} T_7 = 37.38\ Nm$

Common Shaft: $T_{sprocket} = T_9 = T_4 + T_8 = 41.22\ Nm$

$T_{10} = \frac{1}{18/19} T_9 = 43.51\ Nm \rightarrow T_{11} = T_{10} = 43.51\ Nm \rightarrow\ T_{12} = \frac{1}{1/3} T_{10} = 130.53\ Nm$

Component Sizing Analysis

Given that spur gears were chosen for the design, the interference equations were used to determine the upper and lower bounds of the gear sizing in terms of the number of teeth to achieve the required reduction ratios across the drivetrain. The three equations used in this analysis are listed as Equations 11, 12, and 13 below. These equations were simplified by setting k=1 for full-depth teeth and assuming a pressure angle of 20 degrees, as this is the most common pressure angle (23). Full-depth teeth are to be chosen due to many factors, including strength, resistance to wear, contact ratio, and stress. Full-depth teeth have better load distribution,

resulting in greater strength, wear resistance, and stress. They also tend to have a higher contact ratio, meaning more teeth are in contact simultaneously, which is advantageous as it creates smoother operation and reduces noise across the drivetrain.

$$\phi = 20°, k = 1$$
$$N_p = \frac{2}{(1+2m)\sin^2 20°}\left(m + \sqrt{m^2 + (1+2m)\sin^2 20°}\right) \quad (11)$$

$$N_G = \frac{N_p^2 \sin^2 20° - 4}{4 - 2N_p \sin^2 20°} \quad (12)$$

$$m = \frac{1}{VR} \quad (13)$$

In the above equations, N_p represents the smallest number of teeth that will not have interference, N_G represents the largest gear with a specified interference-free pinion, and m represents the reduction ratio. These equations were used in an Excel spreadsheet for each value of m in the drivetrain and are tabulated in Table 5 below.

Table 5: N Values for Reduction Ratios to Reduce Spur Gear Interference.

VR	**2.5:1**	**1:2**	**1:3**
m (1/VR)	**2.5**	**2**	**3**
$\boldsymbol{N_p}$	15	15	15
$\boldsymbol{N_G}$	45	45	45

This table indicates that for all three spur gear ratios, 2.5:1, 1:2, and 1:3, the smallest gear must be 15 teeth or larger, and the larger gear must be 45 teeth or smaller. Using this information, the following gear sizes were selected per component to achieve the necessary reduction ratios for each gear pair with these bounds, shown in Table 6.

Table 6: Chosen Number of Teeth (N) per Component.

Component No.	Component Type	N (Teeth)	Max or Min	Chosen N	VR
1	Spur Gear	15	Min	15	1:3
2	Spur Gear	45	Max	45	
3	Spur Gear	15	Min	20	1:2
4	Spur Gear	45	Max	40	
5	Spur Gear	45	Max	45	2.5:1
6	Spur Gear	15	Min	18	
7	Spur Gear	45	Max	45	2.5:1
8	Spur Gear	15	Min	18	
9	Sprocket	18	N/A	18	18:19
10	Sprocket	19	N/A	19	
11	Spur Gear	15	Min	15	1:3
12	Tire Gear	45	Max	45	

It is also noted that the smallest recommended sprocket size for an electric bicycle is 17, thus these components were set to 18 and 19 to achieve the 18:19 reduction ratio. The component sizes are labeled in Figure 6 below.

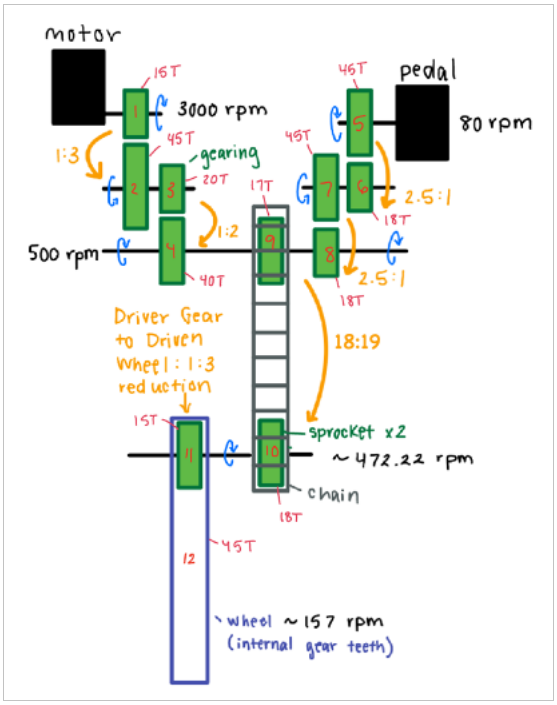

Figure 6: Gear and Sprocket Sizing Based on Interference Equations and VR.

Component Selection & Strength Analysis

Gears and sprockets were selected from transmission catalogs based on strength. Because all shafts in the design are parallel, spur gears were chosen because they do not produce axial thrust. Sprockets manufactured for 0.5" chain pitch were sought, as #40 roller chains are standard for bicycles (20). The Lewis Equation, numbered 14-15, was used to determine the maximum bending stress faced by each gear and sprocket assigned an arbitrary—but standard—pitch diameter.

$$\sigma = \frac{K_v W^t}{FmY}$$
$$F = face\ width,\ m = module$$
$$Y = Lewis\ form\ factor \tag{14}$$

$$K_v = \sqrt{\frac{5.56 + \sqrt{V}}{5.56}}$$
$$K_v \equiv\ velocity\ factor,\ ground\ profile$$
$$V = pitchline\ velocity \tag{15}$$

All components were selected from hardened 1045 carbon steel and SCM415 alloy steel, both common materials for gears. The yield strengths of 1045 steel and SCM415 were found to be 550 and 415 MPa, respectively (1, 25). If the ratio of yield strength to maximum allowable stress for a component exceeded the FOS of 2.52, the component was documented and used in the final design. If the FOS was not met, and because the number of teeth were constrained from interference avoidance, diametral pitch was the specification increased until allowable stress was reduced to an acceptable value. Then a corresponding catalog component could be selected. An example of this analysis for Gear 5 is shown below. This analysis was conducted for all of the gear components.

Assumptions:

pitch diameter $d = 90\,mm;\ F = 20\,mm;\ n = 80\,rpm;\ W^t = 3461\,N;\ Y = 0.399$

$$m = \frac{d}{N} = \frac{90}{45} = 2\,mm$$

$$V = \pi \cdot 80 \cdot 90 \cdot 10^{-3} = 22.619\ \frac{m}{s}$$

$$K_v = \sqrt{\frac{5.56 + \sqrt{22.619}}{5.56}} = 1.362\ \frac{m}{s}$$

$$\sigma = \frac{1.362 \cdot 3461}{20 \cdot 10^{-3} \cdot 2 \cdot 10^{-3} \cdot 0.399} \cdot 10^{-6} = 295.400\ MPa$$

$$SCM415{:}\ S_y = 415\ MPa$$

$$\eta = \frac{415}{295.4} = 1.405 < 2.52$$

Desired FOS not met. Must increase the pitch diameter.

New Assumptions: pitch diameter: $d = 135\,mm;\ F = 30\,mm$

$$m = \frac{d}{N} = \frac{135}{45} = 3\,mm$$

$$V = \pi \cdot 80 \cdot 130 \cdot 10^{-3} = 33.929\ \frac{m}{s}$$

$$K_v = \sqrt{\frac{5.56 + \sqrt{33.929}}{5.56}} = 1.431\ \frac{m}{s}$$

$$\sigma = \frac{1.431 \cdot 3461}{30 \cdot 10^{-3} \cdot 3 \cdot 10^{-3} \cdot 0.399} \cdot 10^{-6} = 137.923\ MPa$$

$$\eta = \frac{415}{137.923} = 3.001 > 2.52$$

Desired FOS exceeded. These gear dimensions and material properties can be used.

KHK and Grainger catalog drawings of selected gears and sprockets appear in Figures 7 through 14, below (11, 26).

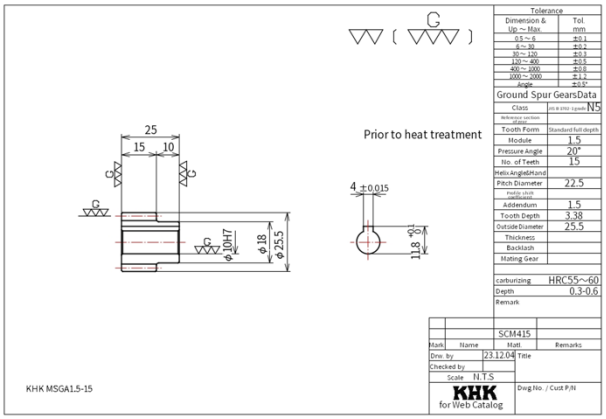

Figure 7: Spur Gear 1
Module 1.5, 15 tooth, Alloy Steel

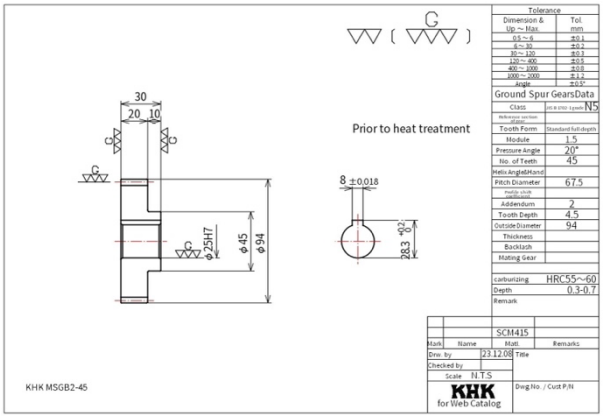

Figure 8: Spur Gear 2
Module 1.5, 45 tooth, Alloy Steel

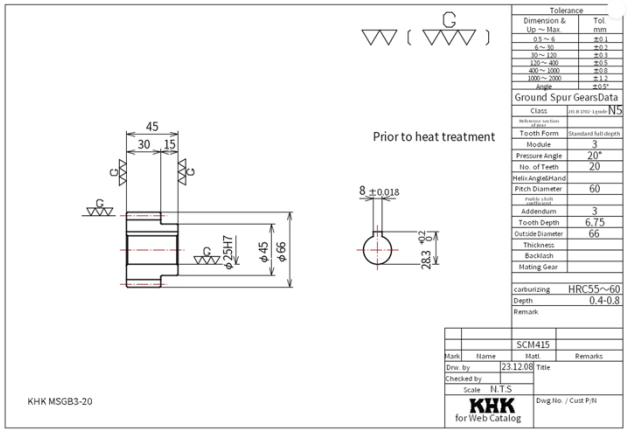

Figure 9: Spur Gear 3
Module 3, 20 tooth, Alloy Steel

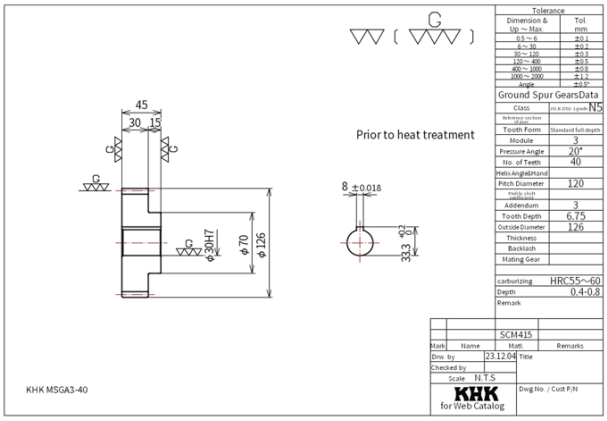

Figure 10: Spur Gear 4
Module 3, 40 Tooth, Alloy Steel

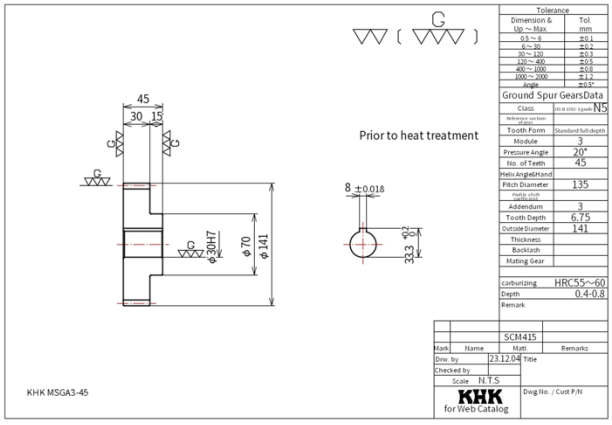

Figure 11: Spur Gears 5,7
Module 3, 45 Tooth, Alloy Steel

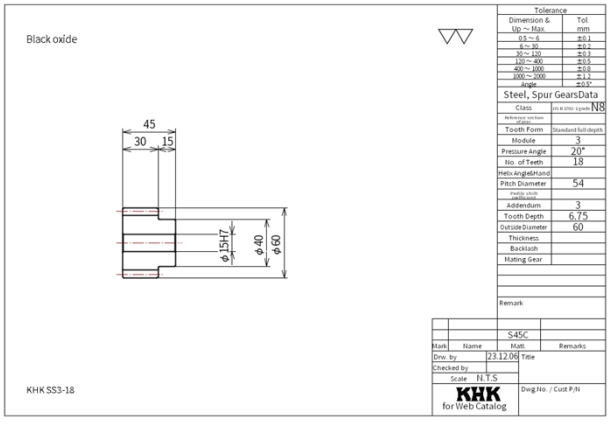

Figure 12: Spur Gears 6,8
Module 3, 18 Tooth, Carbon Steel

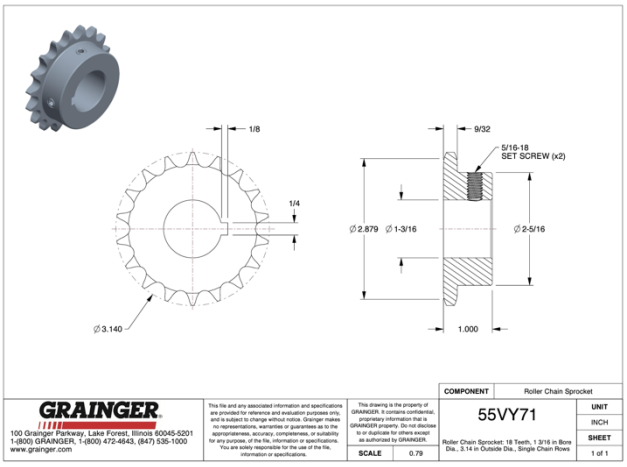

Figure 13: Sprocket 9
0.5” Chain Pitch, 18 Teeth, Carbon Steel

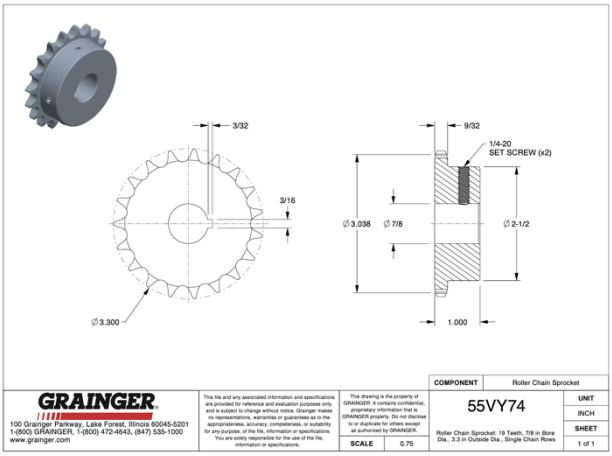

Figure 14: Sprocket 10
0.5” Chain Pitch, 19 Teeth, Carbon Steel

The final velocity reduction from the shaft of Sprocket 10 to the rear wheel was done with a gear. Because the change in velocity is proportional to the change in pitch diameter, the gear had to be a third of the diameter of the wheel, making it rather large at 210mm in diameter. However, the shaft containing this gear and Sprocket 10 is only 20mm in diameter. Gears as large as the one needed are not manufactured with a standard bore size this small, so it is necessary to order a custom part. The rear wheel itself contains internal gearing, which also requires custom manufacturing. The custom gears designed in SolidWorks can be seen in Figures 15 and 16 below.

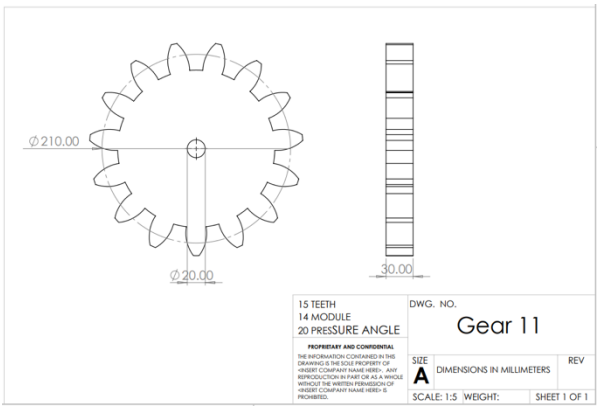

Figure 15: Gear 11
Module 14, 15 Tooth, Alloy Steel

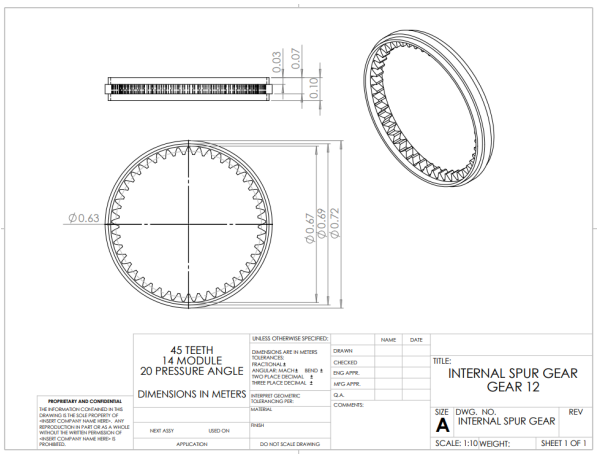

Figure 16: Gear 12
Module 14, 45 Tooth, Alloy Steel

Component Force Analysis

Using the torque values, T, for each component and the pitch radius, r, of each spur gear selected, the forces in each spur gear were calculated using Equations 16 and 17 below. The pressure angle of the spur gears is consistently 20 degrees. A constant pressure angle is critical as it ensures that all of the gears engage smoothly, minimizing noise during operation. The chosen pressure angle of 20 degrees is a standard angle used in gear design that is typically manufactured using standard cutting tools and processes, which simplifies the manufacturing process.

$$T = W_t * r \tag{16}$$

$$W_r = W_t \tan\phi = W_t \tan 20° \tag{17}$$

The spur gears have tangential and radial components to the overall force exerted on the gears, caused by the pressure angle of 20 degrees and the transmission of torque during the interaction of the gear teeth. The tangential force is responsible for the rotational motion of the gears, whereas the radial force component is a result of the meshing action of the gear teeth. This radial force contributes to the radial load on the bearings and shafts that support the gears and is a relevant parameter for analysis and component selection of the bearings and shafts. A diagram including the method for calculating the forces on the gears can be seen in Figure 17 below. The same method was followed for all of the gears within the drivetrain.

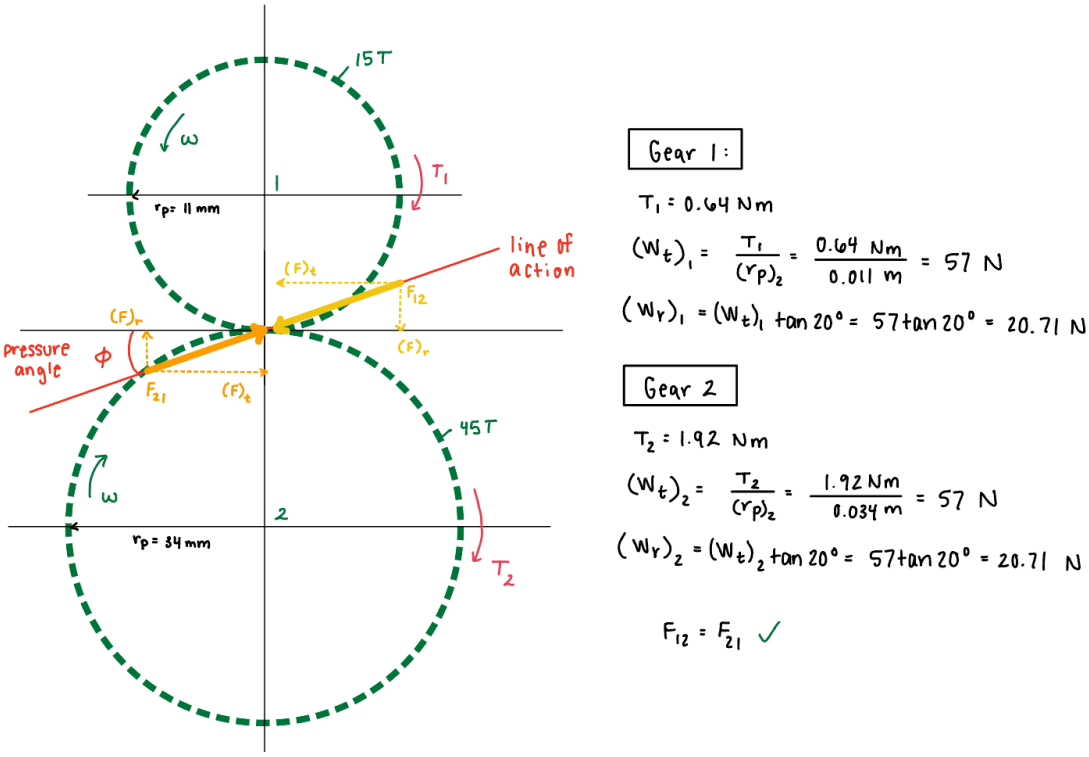

Figure 17: Calculation of Gear Forces for Gears 1 and 2.

A summary of the results of all the force calculations can also be seen in Table 7 below.

Table 7: Tangential and Radial Forces on all Gears in the Drivetrain.

Component No.	Component Type	Torque (Nm)	Wt (N)	pitch radius (mm)	pitch radius, r (m)	Wr (N)
1	Spur Gear	**0.64**	57	11	0.011	20.71
2	Spur Gear	**1.92**	57	34	0.034	20.71
3	Spur Gear	**1.92**	64	30	0.030	23.29
4	Spur Gear	**3.84**	64	60	0.060	23.29
5	Spur Gear	**233.63**	3461	68	0.068	1259.77
6	Spur Gear	**93.45**	3461	27	0.027	1259.74
7	Spur Gear	**93.45**	2077	45	0.045	755.84
8	Spur Gear	**37.38**	1384	27	0.027	503.90
11	Spur Gear	**43.51**	414.38	105	0.105	150.82
12	Internal Tire Gear	**130.53**	414.38	315	0.315	151

To calculate the force in the chain, using Equation 18, the pitch diameter of the sprocket had to be calculated using Equation 19.

$$F_{chain} = \frac{T}{PD/2} \tag{18}$$

$$PD = \frac{P}{\sin 180/N} \equiv pitch\ diameter\ of\ sprocket \tag{19}$$
$$N = \#\ teeth, P = pitch$$

The pitch diameter of the sprockets, components 9 and 10, were found to be 73 mm and 77 mm. Using this information and the torque previously calculated at the sprockets, the force in the chain is 1,127 N. Table 8 below shows the final forces on each sprocket.

Table 8: Force in the Chain Connecting Sprocket Components 9 and 10.

Component No.	Component Type	Torque (Nm)	pitch radius (mm)	pitch radius, r (m)	Fchain (N)
9	Sprocket	41.22	37	0.037	1127.0
10	Sprocket	43.51	39	0.039	1127.0

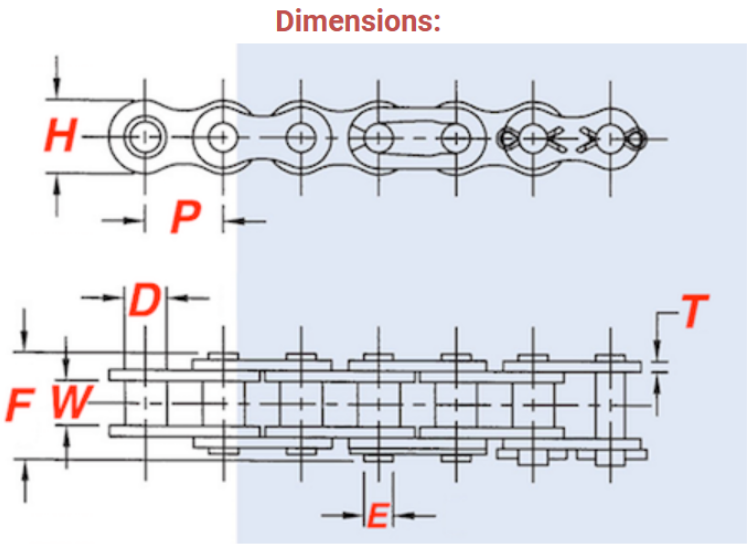

P: 0.500”
W: 0.312”
R: 0.312”
H: 0.463”
T: 0.060”
D: 0.156”
F: 0.640”

Figure 18: #40 Roller Chain Specifications

Before sourcing a roller chain linking the sprockets, the necessary length was found with Equation 20. The SolidWorks assembly was measured in Figure 19 to find the center-to-center distance between the sprockets. The length of the chain was calculated to be 4.64 ft, so a standard 10 ft #40 roller chain with removable links was selected. The catalog tensile strength is 4100 lbs, exceeding our FOS at 3.64 times the designed force in the chain (13).

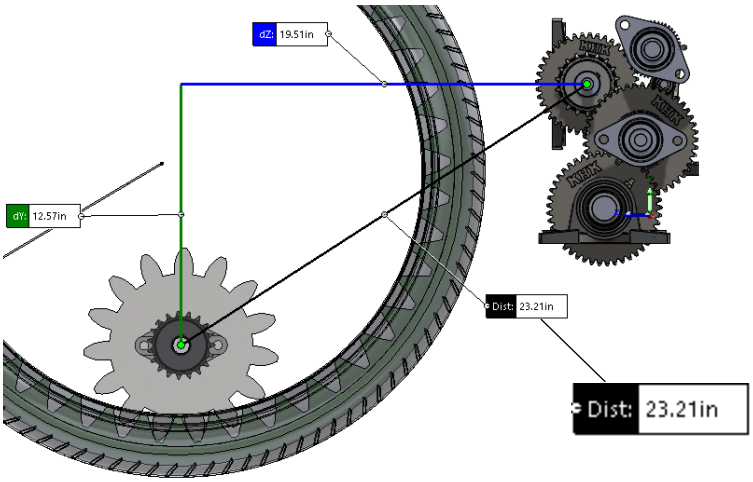

Figure 19: Center-to-Center Distance Between Sprockets

$$\frac{L}{p} \approx \frac{2C}{p} + \frac{N_1 + N_2}{2} + \frac{(N_2 - N_1)^2}{4\pi^2 C/p} \tag{20}$$

$$L - chain\ length \quad p - pitch = .5" \quad C - center\ to\ center$$
$$N_1 - Sprocket\ 9\ Teeth \quad N_2 - Sprocket\ 10\ Teeth$$

Figures 20 and 21 on the next page highlight the placement of the final chain and sprocket system within the full assembly.

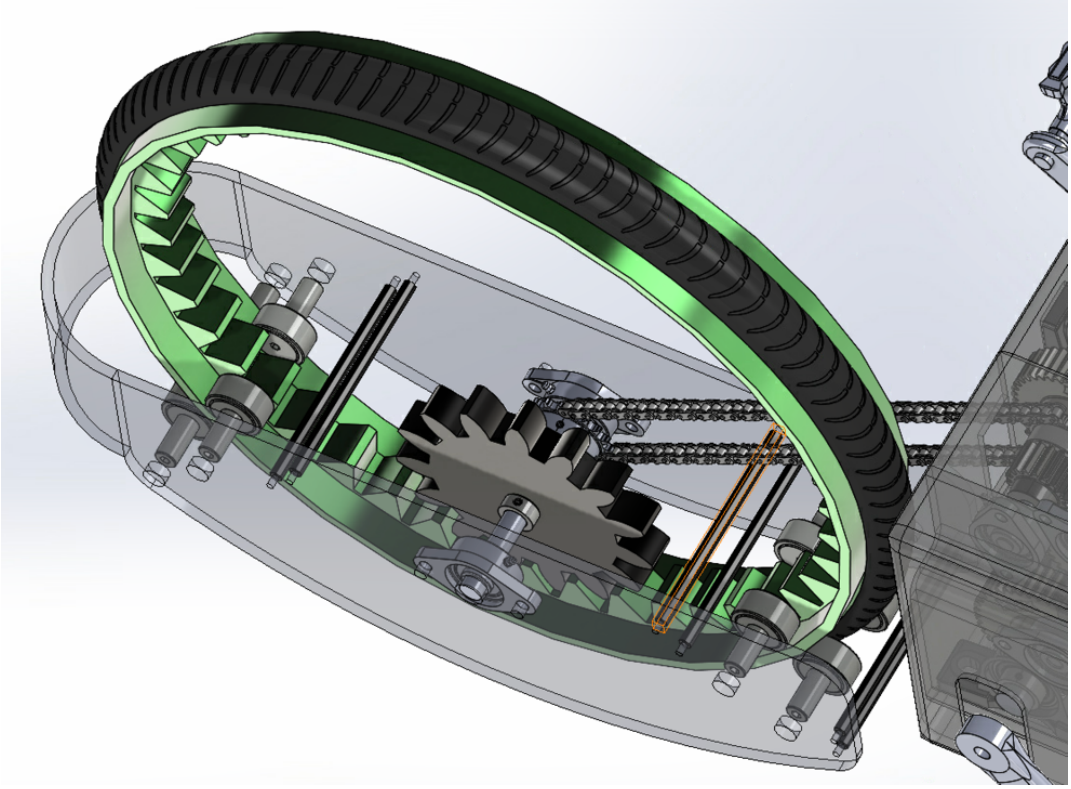

Figure 20: Isometric View of Chain Placement in CAD Model

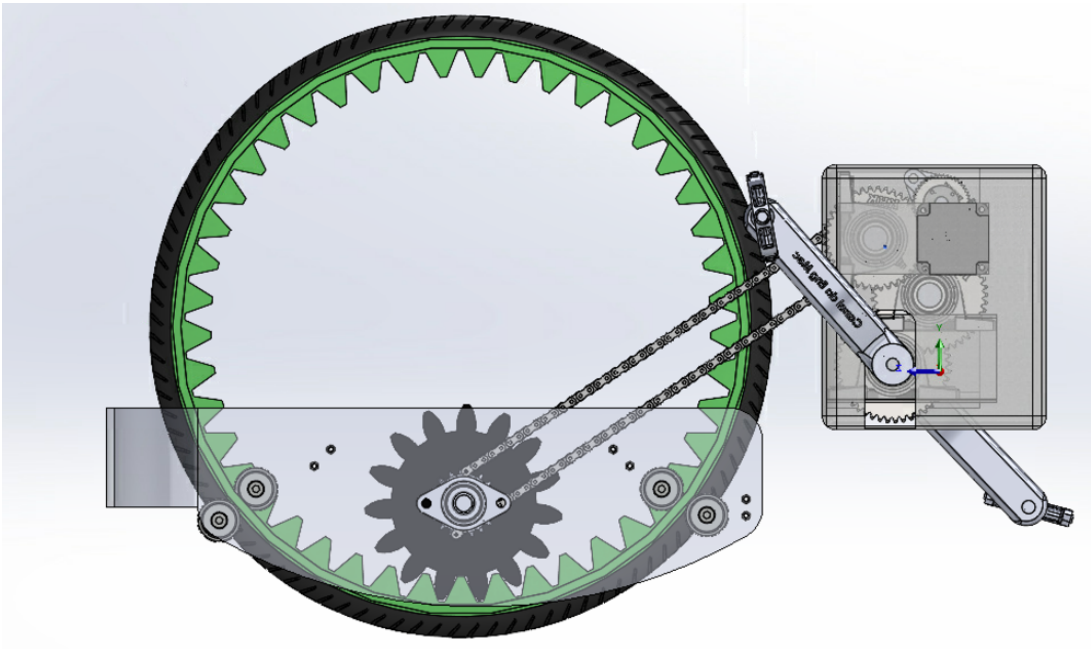

Figure 21: Side View of Chain Placement in CAD Model

Chapter 3: Bearings and Shafts

Bearing Design & Selection

To begin the bearing design process, the resultant force on each bearing was calculated. Figures 19 through 24 below show all math necessary to determine the x and y component of force on each bearing. For consistency across all diagrams, Bearing 1 was the bearing closer to the pedal assembly (right) and Bearing 2 was the bearing closer to the motor (left). Figures 22 through 27 show all calculations performed to determine force on bearings.

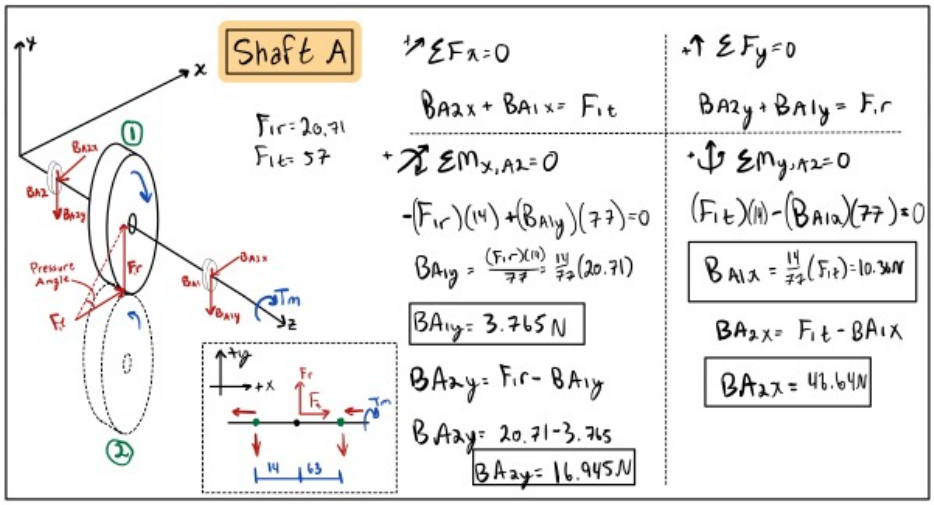

Figure 22: Force Calculations for Shaft A

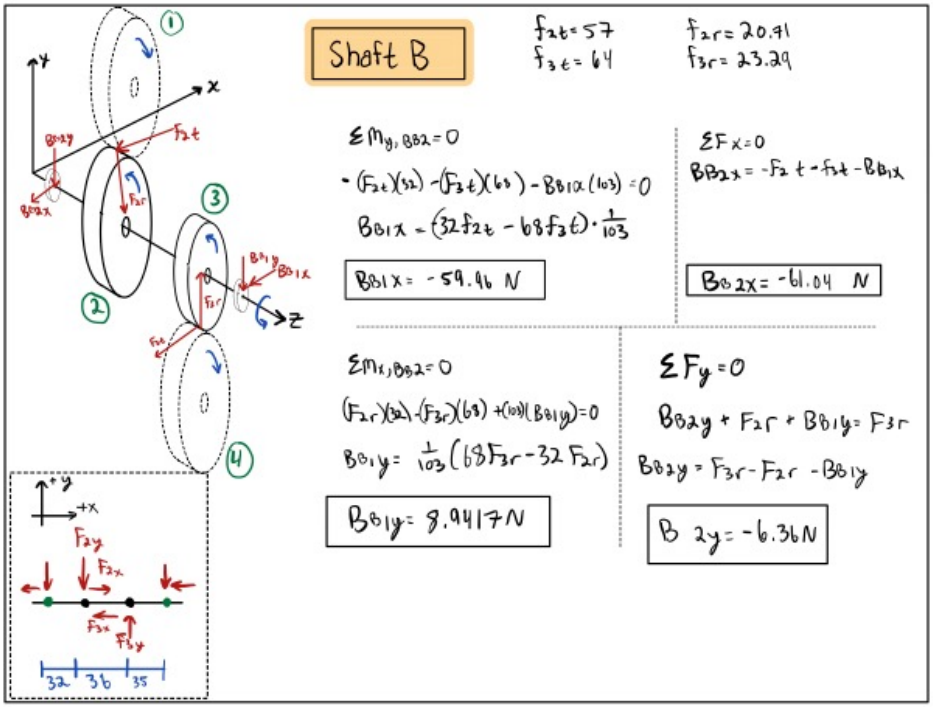

Figure 23: Force Calculations for Shaft B

After Shaft B, the sum of forces in the x and y direction equations were not shown for conciseness.

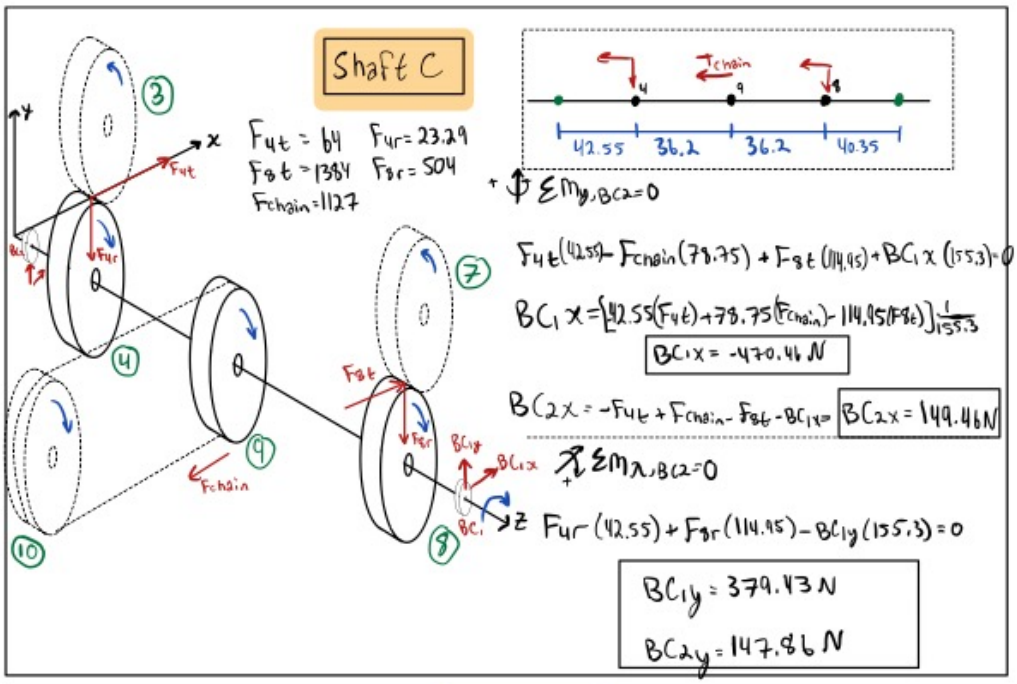

Figure 24: Force Calculations for Shaft C

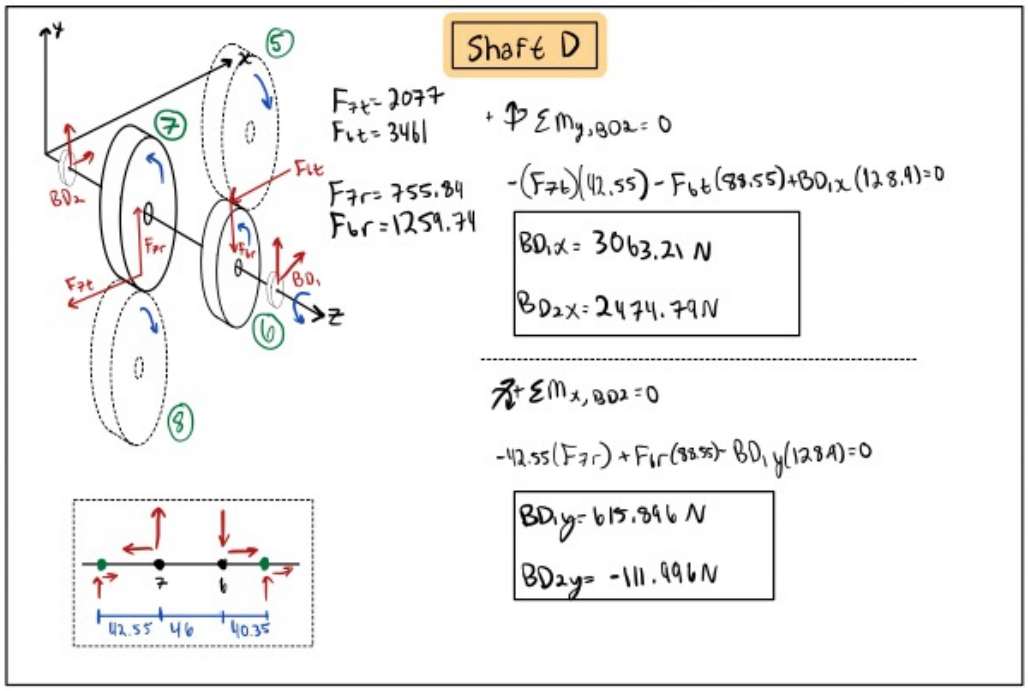

Figure 25: Force Calculations for Shaft D

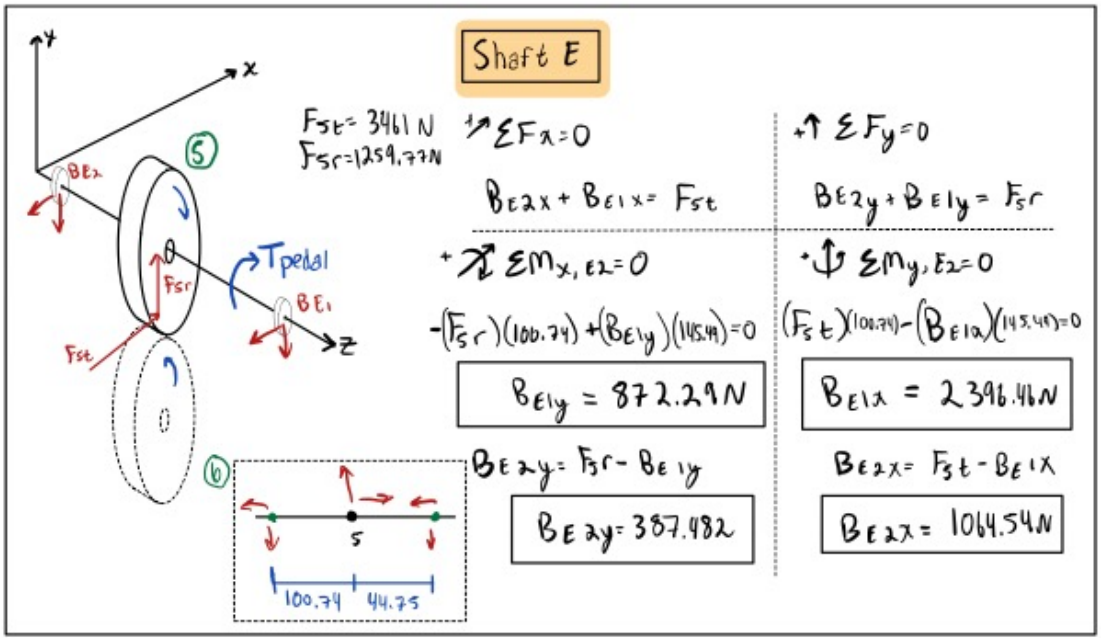

Figure 26: Force Calculations for Shaft E

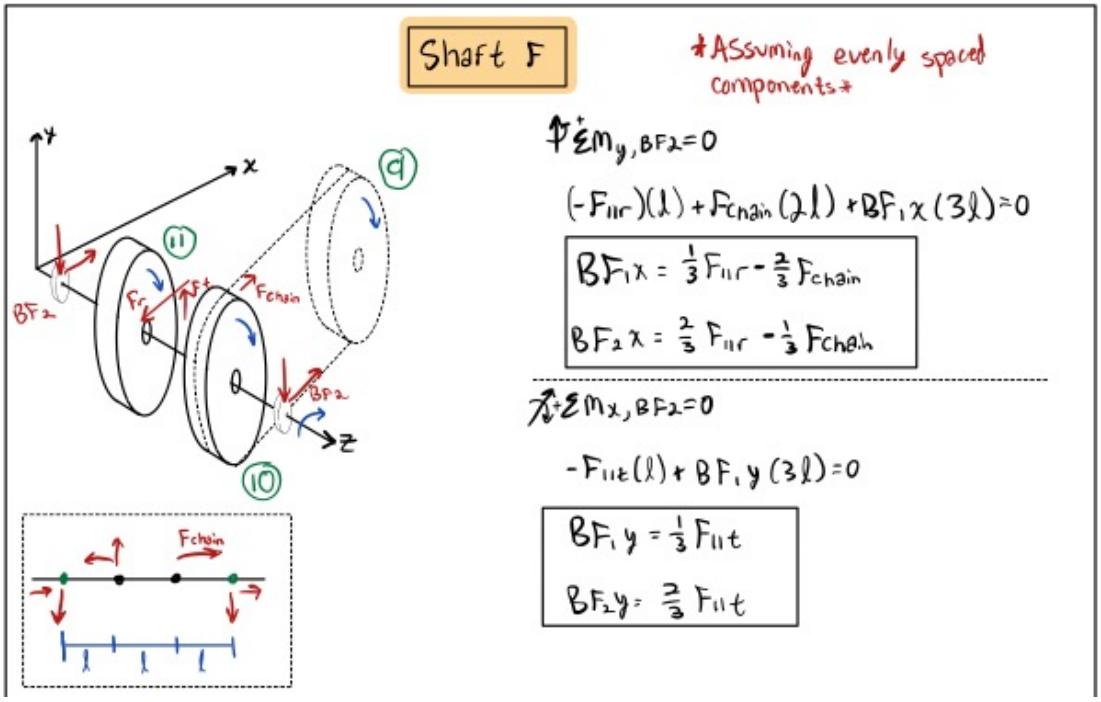

Figure 27: Force Calculations for Shaft F

Equation 21 was used to convert the X and Y components of bearing force into a resultant force. This resultant force is later used in bearing life calculations and catalog selection.

$$F_r = sqrt\left(F_x^2 + F_y^2\right) \tag{21}$$

Table 9 below summarizes all calculated forces on each bearing. Any forces highlighted in red indicate having an opposite direction than the assumed direction in each of Figures 12-27. This opposite-drawn direction, however, does not impact the magnitude of resultant force.

Table 9: Forces On All Shaft Bearings.

Shaft	B1 – X (N)	B1 – Y (N)	B1 – R (N)	B2 – X (N)	B2 – Y (N)	B2 – R (N)
A	10.36	3.77	**11.02**	46.64	16.95	**49.62**
B	-59.96	8.94	**60.62**	-61.04	-6.36	**61.37**
C	-470.46	379.43	**604.40**	149.46	147.86	**210.24**
D	3063.21	615.90	**3124.51**	2474.79	-112.00	**2477.32**
E	2396.46	872.29	**2550.28**	1064.54	387.48	**1132.87**
F	117.91	-708.89	**718.63**	235.83	-290.07	**373.84**

The resultant forces acting on the bearings calculated and listed in Table 9 represents the desired radial load that the selected bearings need to withstand, F_D. The rated load to compare to the catalog dynamic radial load capacities can be calculated using Equation 22 below. The rated life is found in the bearing catalogs to be $1 * 10^6$ revolutions which can be converted to hours using the speeds of the shafts, n, in Equation 23. The desired life, L_D, was set to 12,000 hours for all of the bearings. This life was referenced from the following figure, which recommends 12,000 hours for "intermittent operation during the day, reliability important" (5).

Operating Condition	Minimum L10 Life (Hours)
Intermittent operation during day, service interruptions acceptable	8,000
Intermittent operation during day, reliability important	12,000
Continuous 1 shift operation	20,000
Continuous 2 shift operation	40,000
Continuous 24 hour operation	60,000
Continuous 24 hour operation reliability important	100,000

Figure 28: Suggested Minimum Bearing Rating Lives for Various Operating Conditions.

$$F_R = F_D \left(\frac{L_D}{L_R}\right)^{\frac{1}{a}} \tag{22}$$

$$L_R = \frac{10^6}{60n} \tag{23}$$

The next page includes an example calculation of the load and life calculations for Shaft A, Bearings 1 and 2. The same process was repeated for all bearings and shafts.

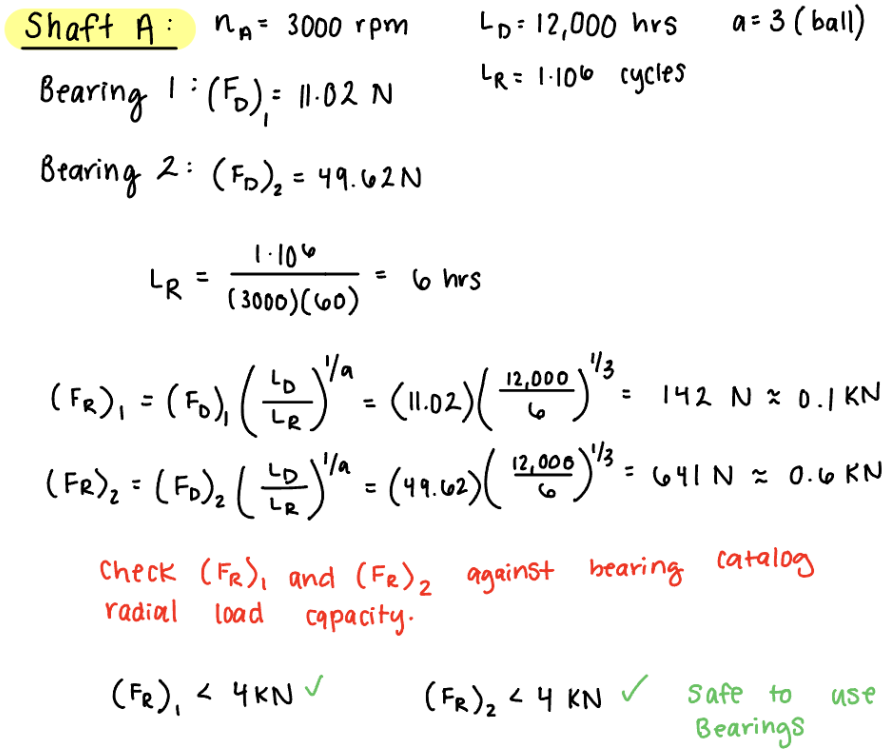

10 mm bore

Product No. KP	Product No. SSKP	No.	d mm	a mm	b mm	e mm	g mm	h mm	s_1 mm	w mm	L_k mm	n_k mm	Bearing-Load Rating[1) KP dyn. C kN	KP stat.C_0 kN	SSKP dyn. C kN	SSKP stat.C_0 kN	Weight KP g	Weight SSKP g
625 608 00	-	08	8	55	13	42	5	15	4,8	29	11,5	3,5	4,2	1,6		-	70	-
625 610 00	625 996 10	00	10	67	16	53	6	18	7	35	15	4	4,7	2,0	4,0	1,6	60	70
625 612 00	625 996 12	001	12	71	16	56	6	19	7	38	15	4	5,2	2,45	4,4	1,95	70	100
625 615 00	625 996 15	002	15	80	16	63	7	22	7	43	16,5	4,5	5,7	2,9	4,85	2,3	100	140
625 617 00	625 996 17	003	17	85	18	67	7	24	7	47	17,5	5	6,1	3,35	5,2	2,7	130	190
625 620 00	625 996 20	004	20	100	20	80	9	28	10	55	21	6	9,55	5,15	8,1	4,1	190	230
625 625 00	625 996 25	005	25	112	20	90	10	32	10	62	22,5	6	10,3	5,95	8,75	4,75	230	290

Figure 29: Load and Life Calculation for Bearings 1 and 2 on Shaft A.

Table 10 summarizes the radial loads for each bearing that will be used to compare to the catalog bearings to ensure load and life requirements are achieved.

Table 10: Rated Radial Forces Required for Both Bearings on Each Shaft.

					F_R, Rated Force			
					Bearing 1		Bearing 2	
Shaft	L_D	**n (rpm)**	L_R **(hours)**	**a**	**N**	**kN**	**N**	**kN**
A	12000	3000	6	3	142	0.1	641	0.6
B	12000	1000	17	3	543	0.5	550	0.6
C	12000	500	33	3	4300	4.3	1496	1.5
D	12000	200	83	3	16377	16.4	12985	13.0
E	12000	80	208	3	9849	9.8	4375	4.4
F	12000	474	35	3	5021	5.0	2611.9	2.6

After calculating the necessary bearing rated forces, the team was able to begin sourcing bearings. All bearings were initially found without housings. When tasked with integrating the bearings into the overall design it was evident that unsupported bearings could not be used. Pillow and flange blocks were then sourced, given each bearing specification, to be used in the overall design. Pillow blocks were preferred for ease of installation, but for some bearings, such as the 16mm, flange blocks were selected due to availability. Their specifications can be viewed in Figures 30-34 on the next page. Figures 35 through 37 illustrate the gearbox with all bearings added in.

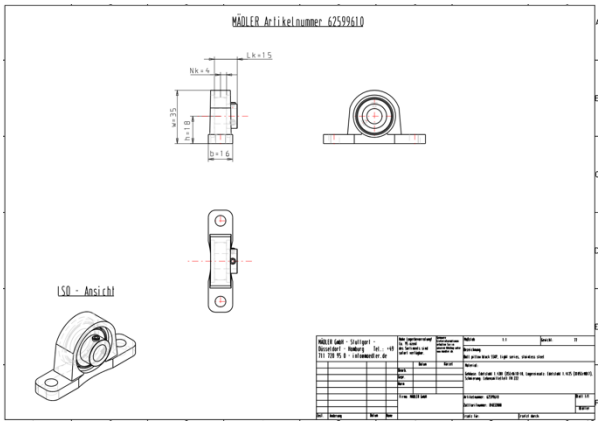

Figure 30: 10mm Pillow Block Ball Bearing

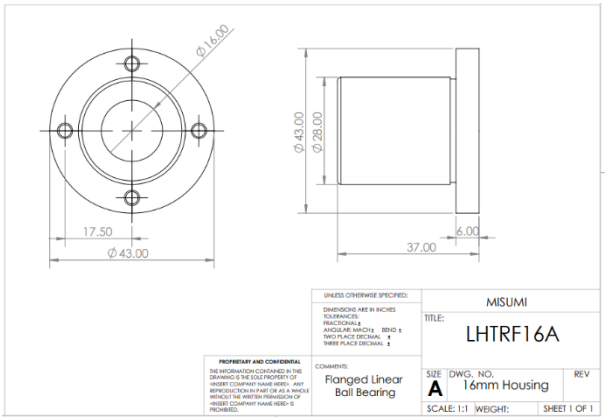

Figure 31: 16mm Flanged Linear Ball Bearing

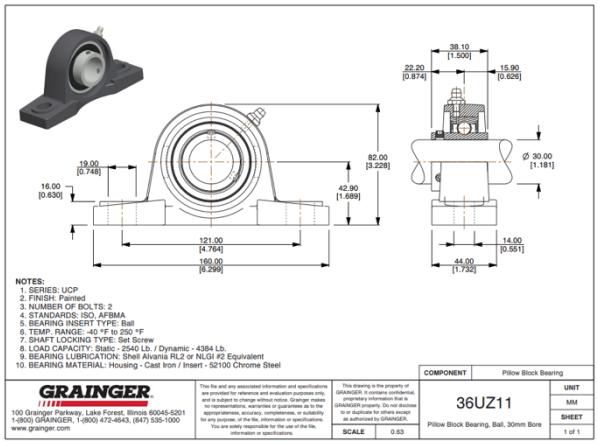

Figure 32: 30mm Pillow Block Ball Bearing

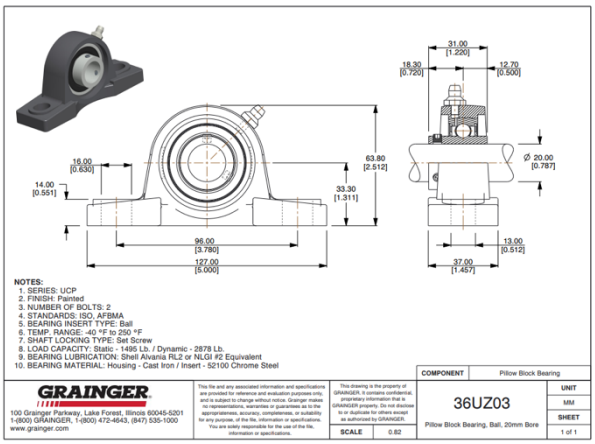

Figure 33: 20mm Pillow Block Ball Bearing

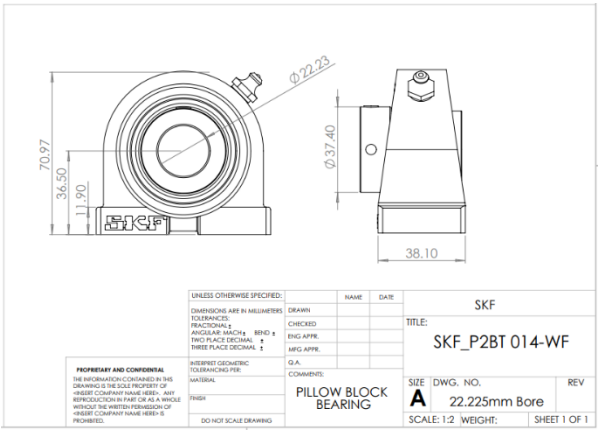

Figure 34: 22.2mm Pillow Block Ball Bearing

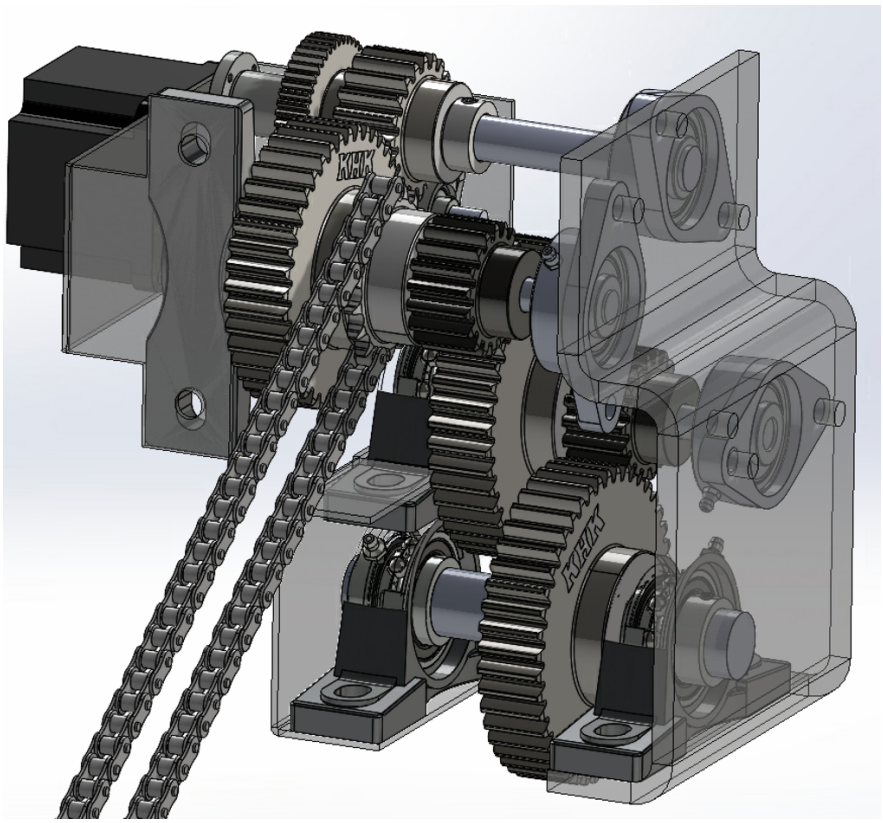

Figure 35: Back View of Gearbox

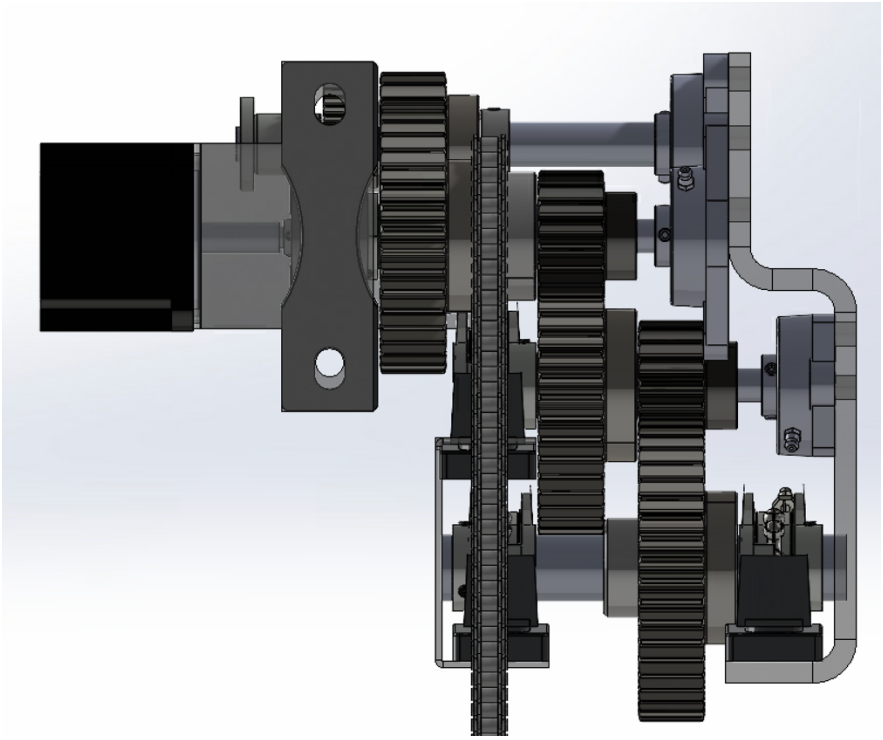

Figure 36: Top View of Gearbox.

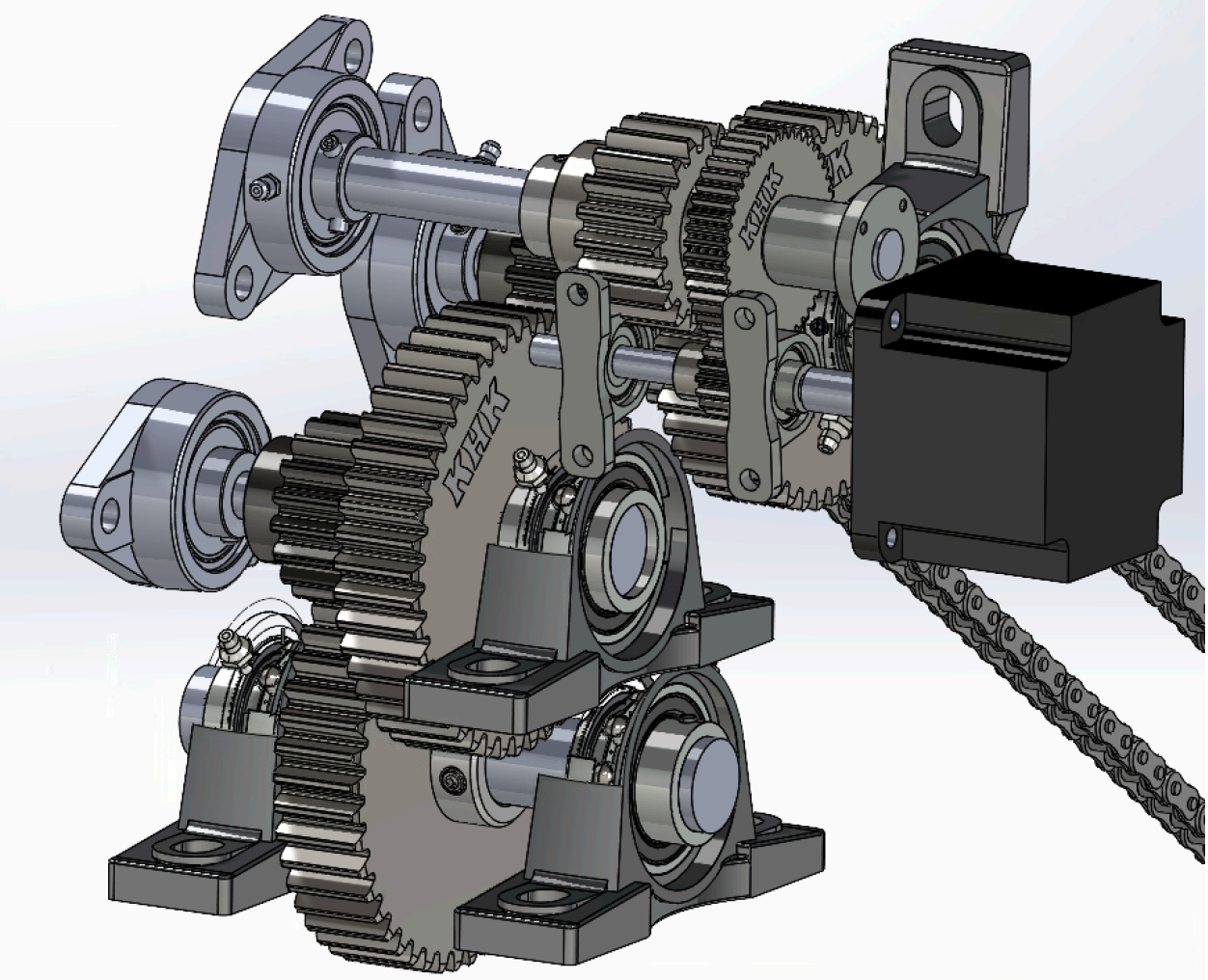

Figure 37: Front View of Gearbox

Shaft Selection

The shaft selection began with finding all forces on the bearings through free body diagram analysis of the shaft. This is shown in the bearing design and selection section above. The spacing of each component was theoretically estimated and later confirmed in the SolidWorks CAD assembly. Next, shear force (SFD) and bending moment diagrams (BMD) were created for each shaft. Figures 38-42 below illustrate all SFD and BMD completed.

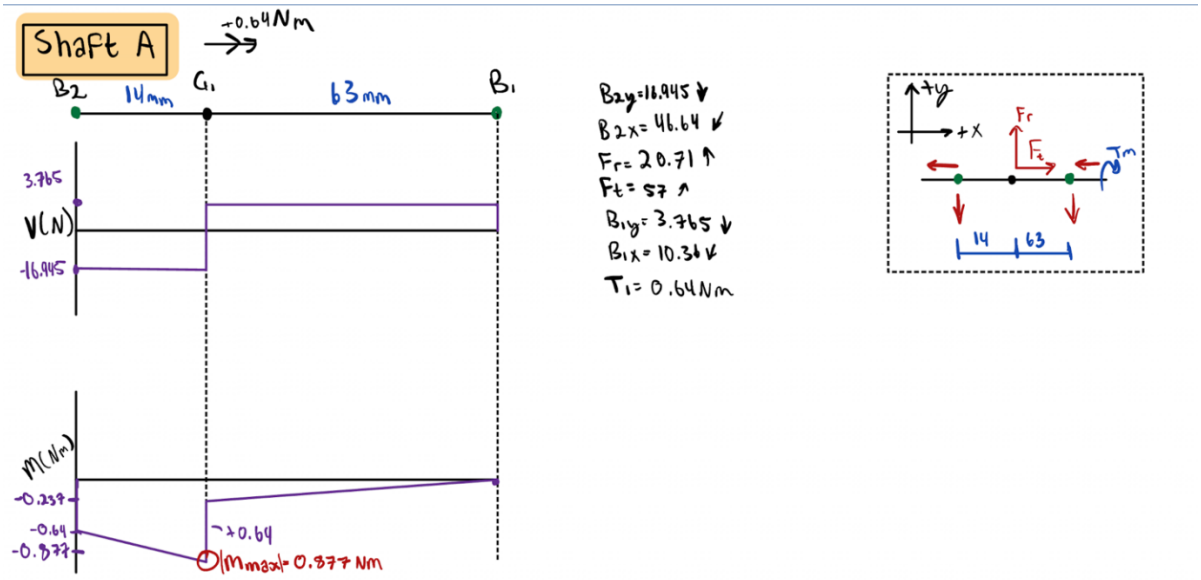

Figure 38: SFD and BMD for Shaft A

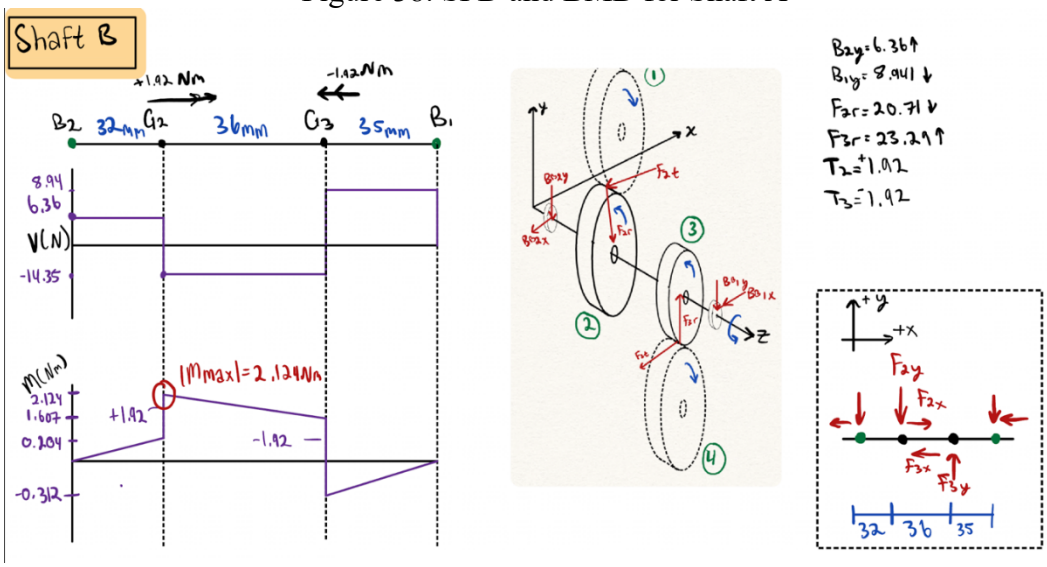

Figure 39: SFD and BMD for Shaft B

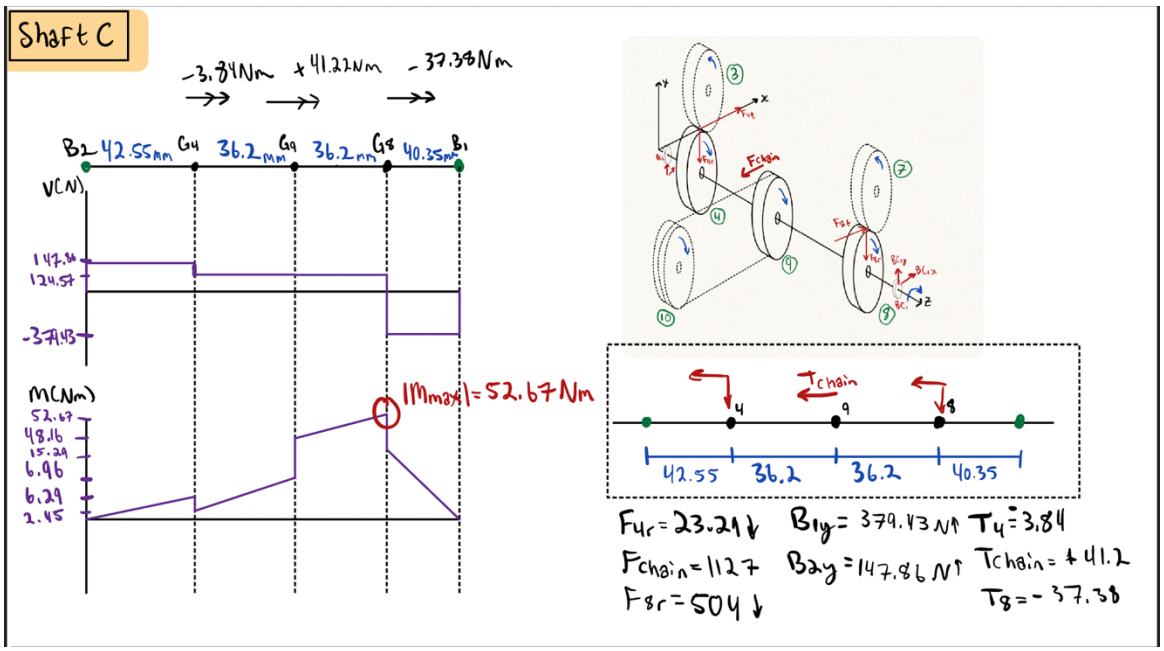

Figure 40: SFD and BMD for Shaft C

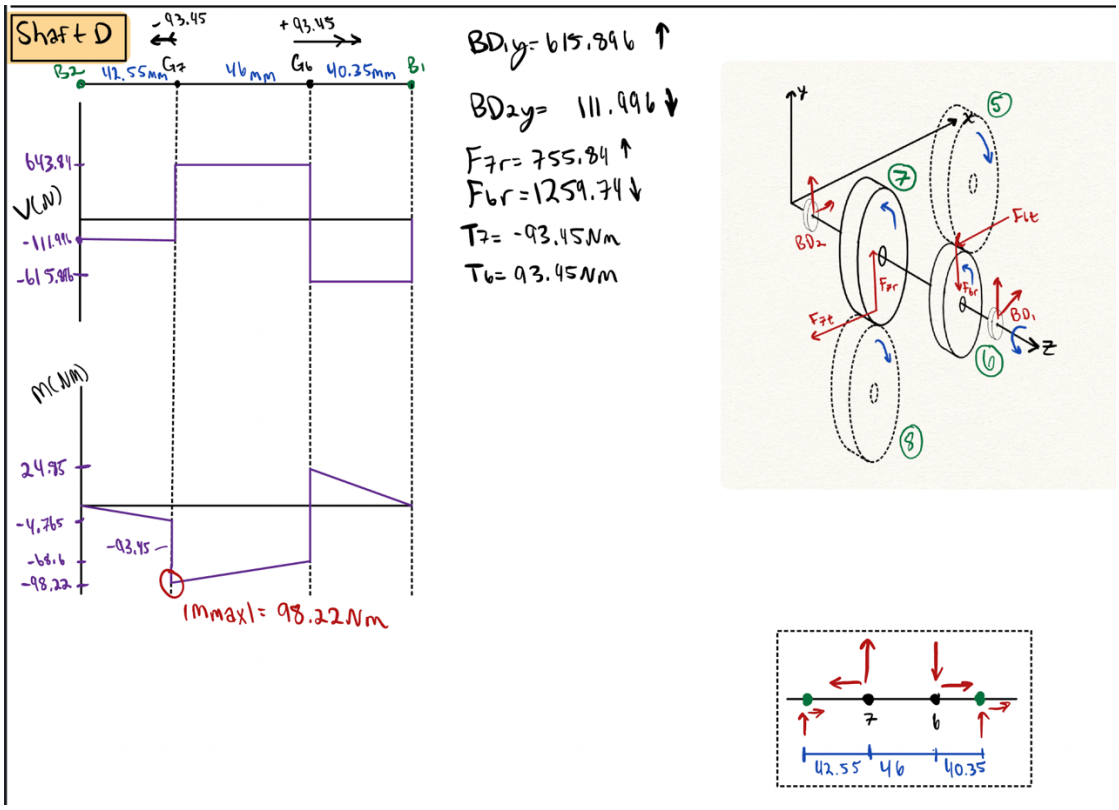

Figure 41: SFD and BMD for Shaft D

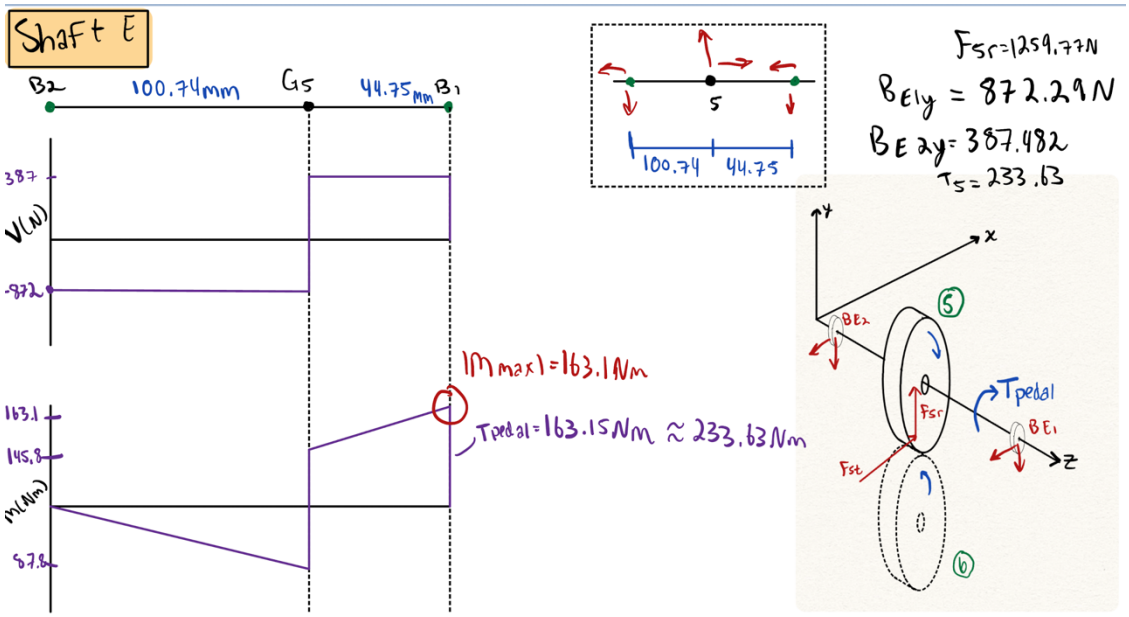

Figure 42: SFD and BMD for Shaft E

Yield strength was then calculated using Equation 24 below. M represents the maximum bending moment, r is the minimum shaft radius, and I is the area moment of inertial.

$$\sigma = \frac{M * r}{I} = \frac{M * r}{\frac{pi}{4} * r^4} \tag{24}$$

Figure 43 below shows a sample calculation of stress on Shaft A.

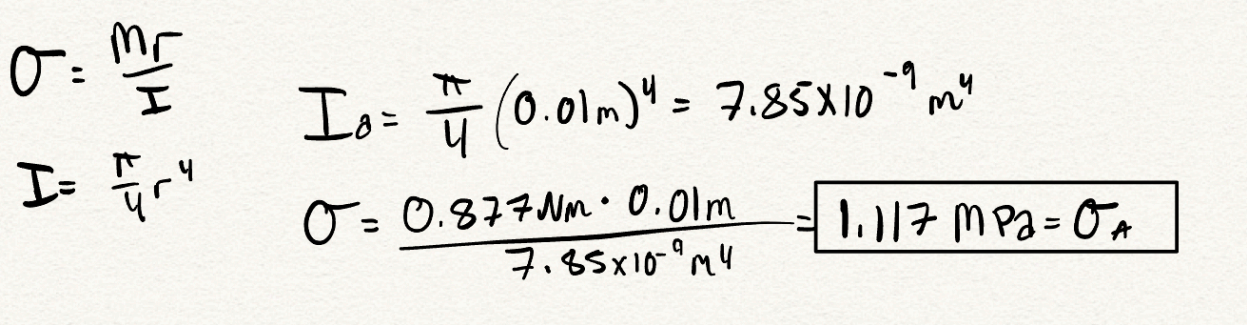

Figure 43: Stress on Shaft A Calculation

Using this method, the yield strength of all shafts was found. Table 11 below illustrates these results.

Table 11: Yield Strength Required In Each Drivetrain Shaft

Shaft	**Max Bending Moment (Nm)**	**Minimum Radius (m)**	**Area Moment of Inertia (m^4)**	**Stress (Mpa)**
A	0.877	0.01	7.85E-09	1.117
B	2.124	0.016	5.15E-08	0.660
C	52.67	0.015	3.98E-08	19.870
D	98.22	0.015	3.98E-08	37.054
E	163.1	0.03	6.36E-07	7.691

As a result, none of the shafts require an exceptionally high yield strength, with the maximum stress being 37.054. To account for differing gear bore diameters, some shafts will be built as step shafts with various diameters, as dimensioned in Figures 44-49. To assist in machining and cost, Aluminum 3003 has been selected as the material for all shafts. This material is easily machinable and has a yield strength of 186 MPa (2). This strength withstands all required in the drivetrain.

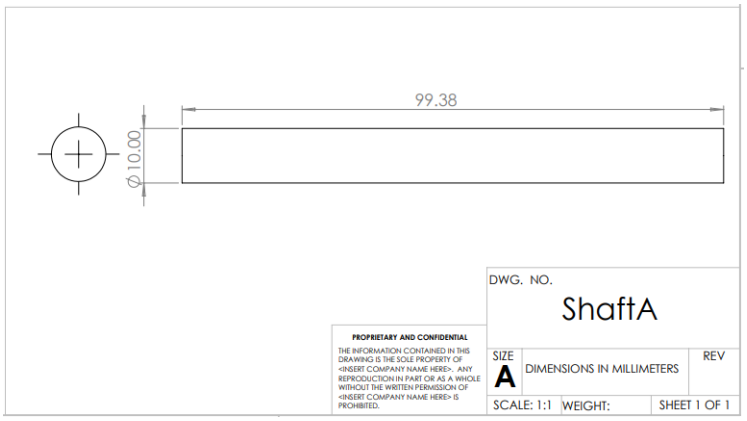

Figure 44: Shaft A Drawing

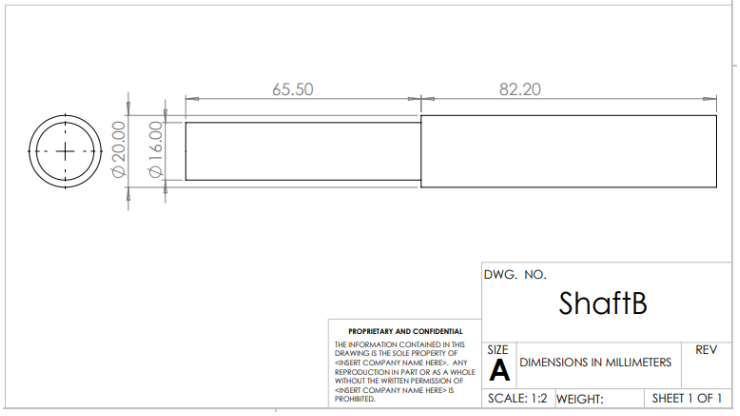

Figure 45: Shaft B Drawing

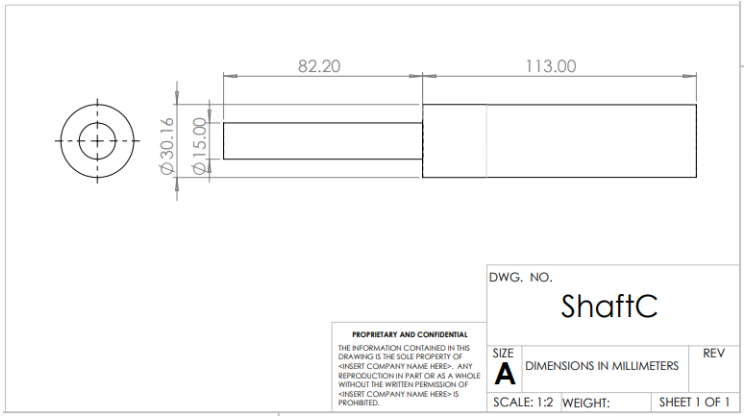

Figure 46: Shaft C Drawing

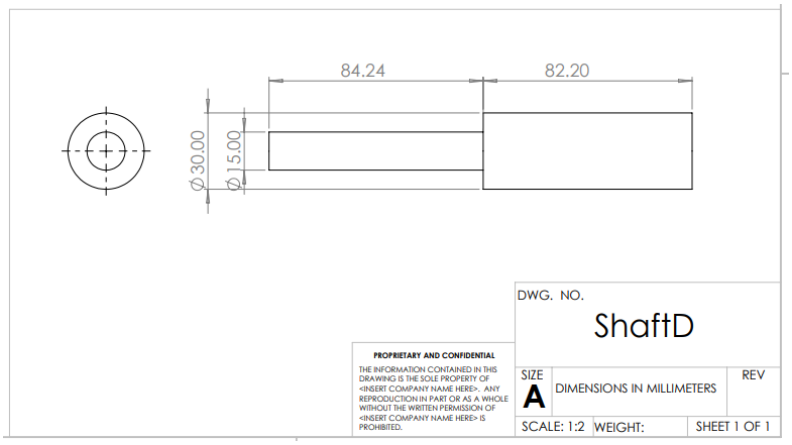

Figure 47: Shaft D Drawing

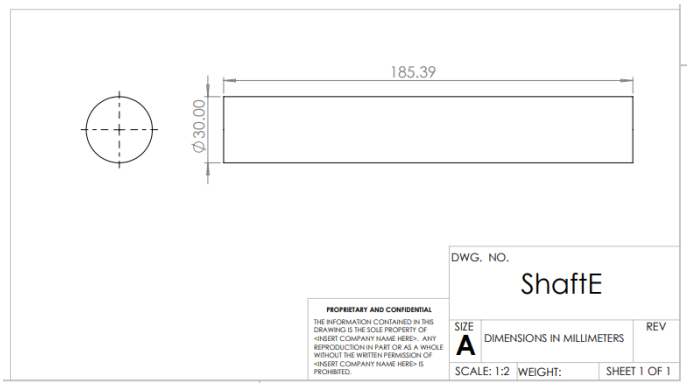

Figure 48: Shaft E Drawing

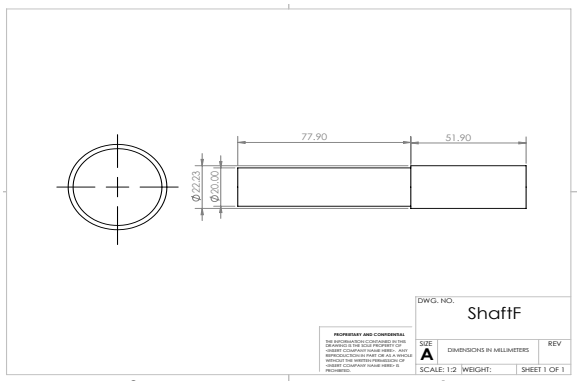

Figure 49: Shaft F Drawing

Chapter 4: Hubless Wheel Bearings

Wheel Support

The rear wheel did not have a hub. Instead, it had to be structurally supported via bearings. These bearings had to be structurally sound and roll smoothly to minimize energy losses due to friction. These bearings had to be small enough to be integrated into the frame-wheel assembly with minimal added space and weight. Fitting these criteria, a needle bearing cam follower from Misumi was chosen, as shown in Figure 50.

Figure 50: Needle Bearing Cam Follower From Misumi.

After the type of bearing was chosen, the location of these bearings relative to the wheel had to be decided. This decision was critical as it determined the torque control the frame had over the wheel, the likelihood for the wheel to warp, and the spatial requirements for the frame. In order to maintain the hubless design, the angle between the outermost bearings had to be 120° or less. However, 120° was also the angle that provided the greatest torque control, so it was chosen for the design. To minimize warping of the rear wheel, it was best to symmetrically mount the bearing supports on the bottom of the wheel, rather than compressing the wheel from above. With these factors in mind, the final bearing arrangement was decided and depicted in Figure 51. The forces on the wheel were then calculated using the free body diagram shown in Figure 52.

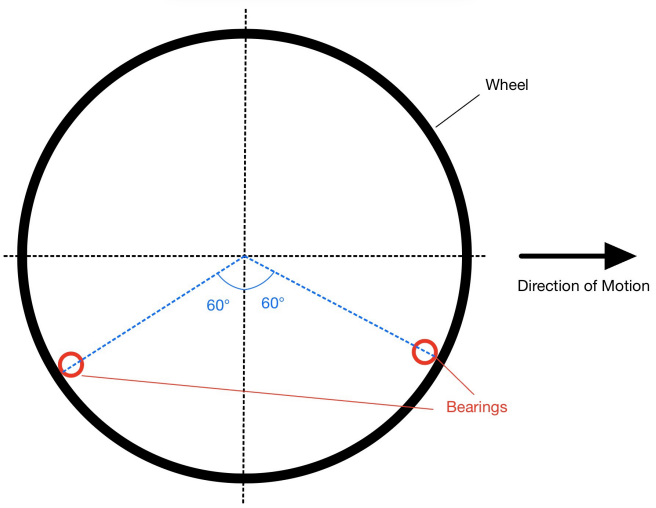

Figure 51: Chosen bearing arrangement on rear wheel

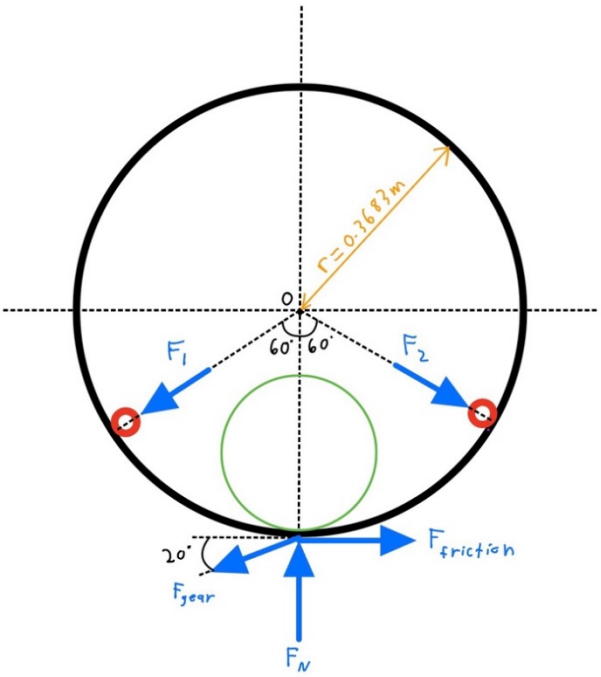

Figure 52: Free Body Diagram of Rear Wheel

In order to maximize the bicycle's ability to roll over obstacles, it was decided that 2/3 of the weight of the rider should be distributed to the rear wheel (30). Since the weight limit of the bicycle was 300 lbs, 200 lbs of force (889.64 N) was loaded onto the rear wheel. The force of the rear spur gear was found using the delivered torque. The weight of the rear wheel was estimated to be 3kg (28) which was neglected since it was insignificant compared to the rest of the weight

of the rider. The diameter of the rear wheel was 29 in, so the radius was 14.5 in (0.368 m). The resultant radial forces acting on the bearings were calculated to be 373.96 N per bearing as shown in Figure 53.

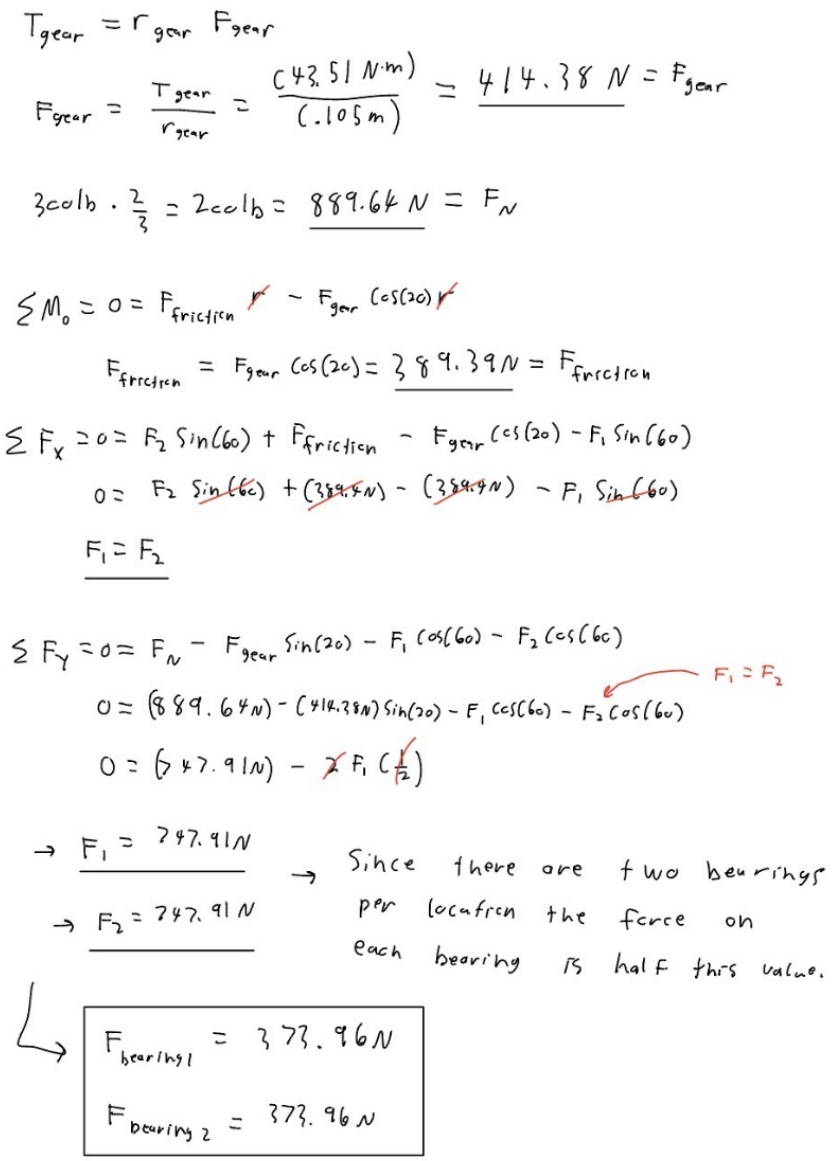

Figure 53: Calculations to Find Radial Force on Wheel Bearings

As described earlier with Figure 26, the desired life of these bearings were 12,000 hours. The Misumi needle cam follower bearing was rated at a dynamic load of 13.4 kN for a life of 10^6 cycles. With a desired load of 373.96 N, the bearing life equations (Equation 22 and Equation

23) were used to determine that the bearings had to be rated for a dynamic load of at least 4993.5 N. These calculations are shown in Figure 54 below. Since this was less than the Misumi dynamic load rating, the Misumi needle cam follower bearings were confirmed to support the rear wheel for at least 12,000 hours.

$$L_R = \frac{10^6}{60n} = \frac{10^6}{60(3304.2\ rpm)} = 5.04\ hr$$

$$L_D = 12000\ hr \qquad a = 3$$

$$F_D = 373.96\ N$$

$$F_R = F_D \left(\frac{L_D}{L_R}\right)^{\frac{1}{a}} = (373.96\ N)\left(\frac{12000\ hr}{5.04\ hr}\right)^{\frac{1}{3}}$$

$$F_R = 4992.5\ N < 13.4\ kN$$

↑ from Misumi

Figure 54: Needed Rating for Wheel Support Bearings

Bearings and Wheel Support

Needle bearing cam followers from Misumi were chosen to support the wheel and connect the wheel to the frame across 120° (6). For the bearings to support the wheel from its outer and inner edges, the physical wheel was designed with grooves to ensure the bearings remain in position. The grooves, being the width of the bearings, allow the bearings to rest on the wheel while obstructing axial movement. An isometric view of the bearings positioned in the wheel grooves is shown below in Figures 55 and 56.

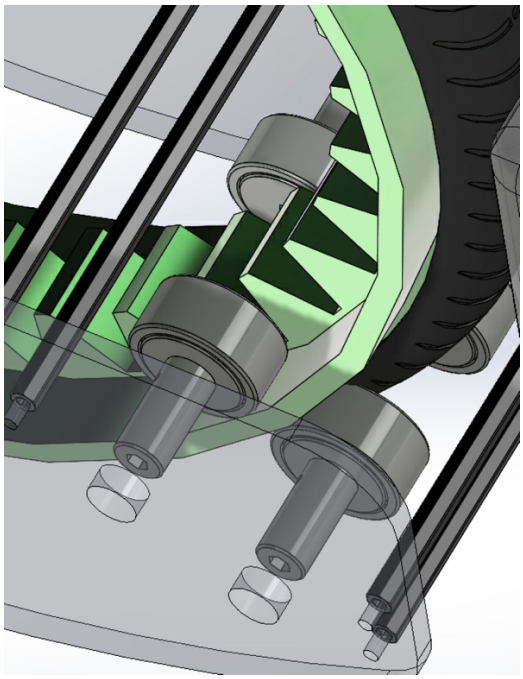

Figure 55: Isometric View of Bearings Positioned on Wheel

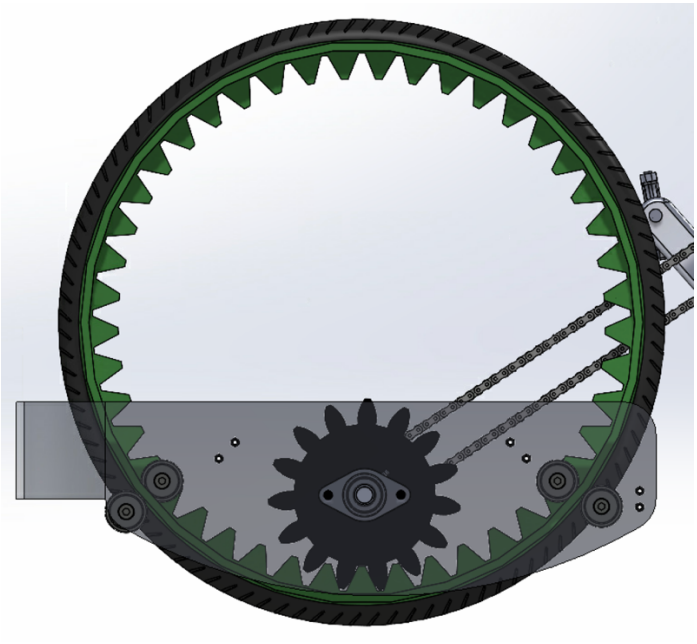

Figure 56: Side View of Bearings Positioned on Wheel

Drivetrain Containment

The motor and component's location were selected to be housed and hidden within the center of the frame. This affords enough space to put the motor, battery, and gear boxes while keeping components hidden to reduce interference with the bike operator and enhance the aesthetics of the overall design. Custom sheet metal framing was designed to seamlessly enclose all components of the drivetrain for an elegant design. All drivetrain components are mounted to these brackets to secure each component to the bike frame. Additionally, mounting the drivetrain low on the frame provides a lower center of gravity; a lower center of gravity enables the bike to be handled more easily on technical terrain (27). Figure 57 below depicts the intended motor and gearbox housing location. A standard bike frame is currently used to represent spacing of all components. With future iterations, however, the frame may be redesigned to better accommodate the gearbox sizing.

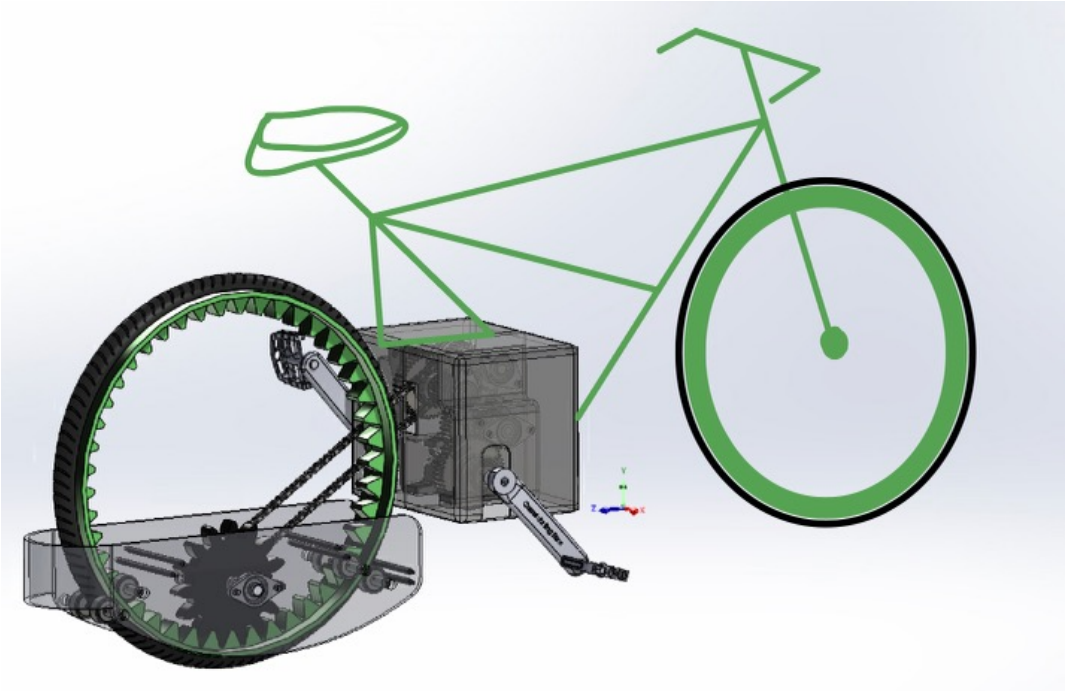

Figure 57: Proposed Frame and Drivetrain Housing

Final Assembly Design

A side view and isometric view of the intended final design are shown below in Figures 58 and 59.

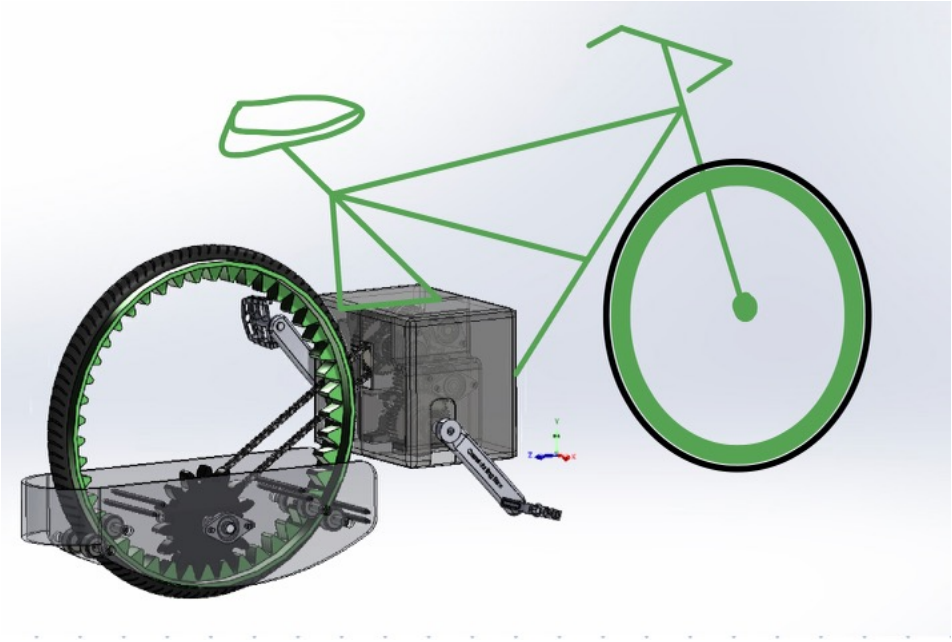

Figure 58: Isometric View of Final Layout

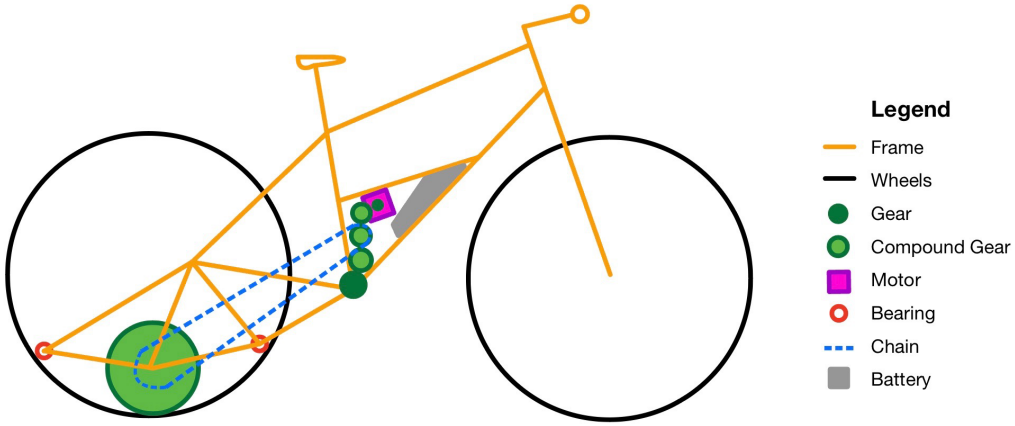

Figure 59: Side View of Final Layout

Below, Figures 60 through 62 illustrate the full assembly.

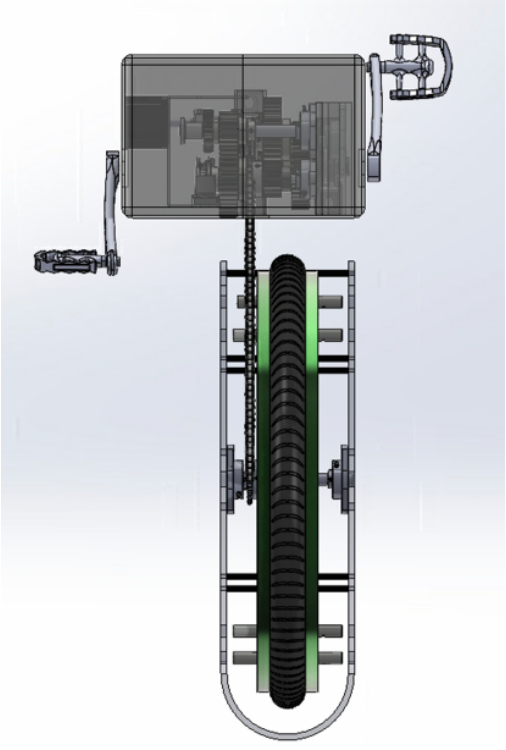

Figure 60: Top view of Final Assembly

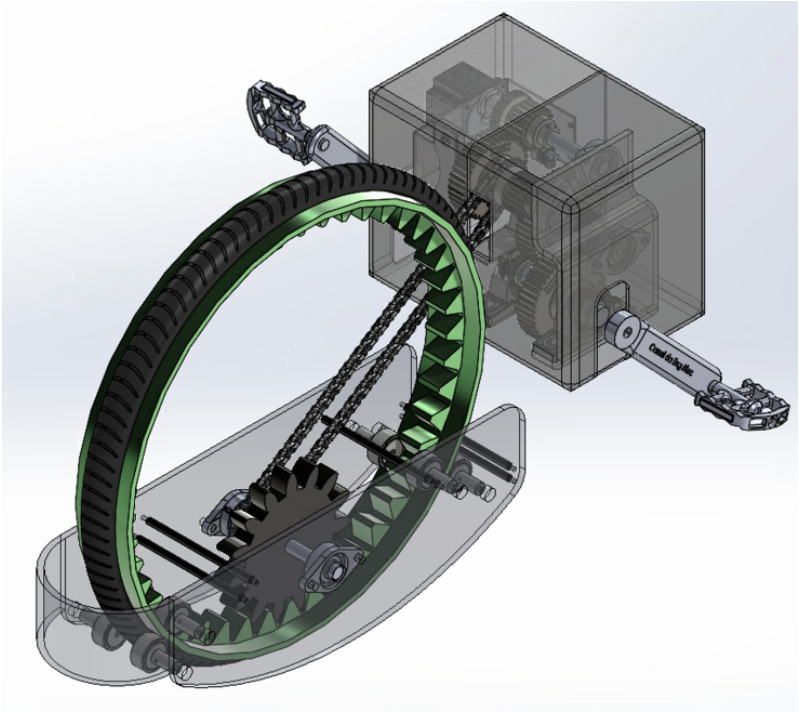

Figure 61: Isometric View of Final Assembly

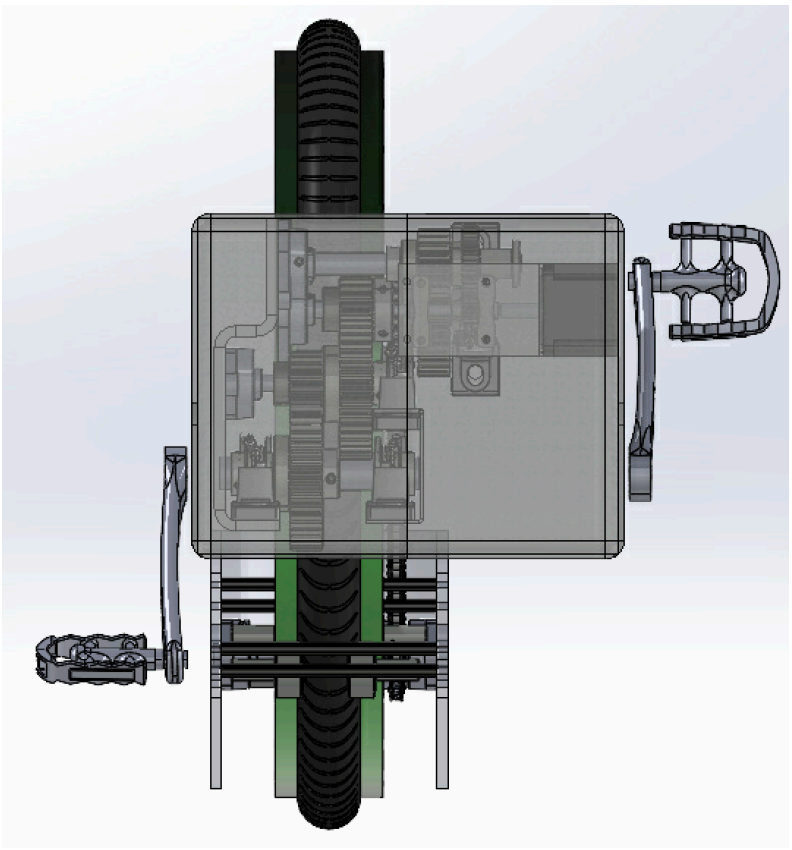

Figure 62: Front View of Final Assembly

Lastly, see Figures 63 through 66 for detailed drawings of all enclosure metal brackets.

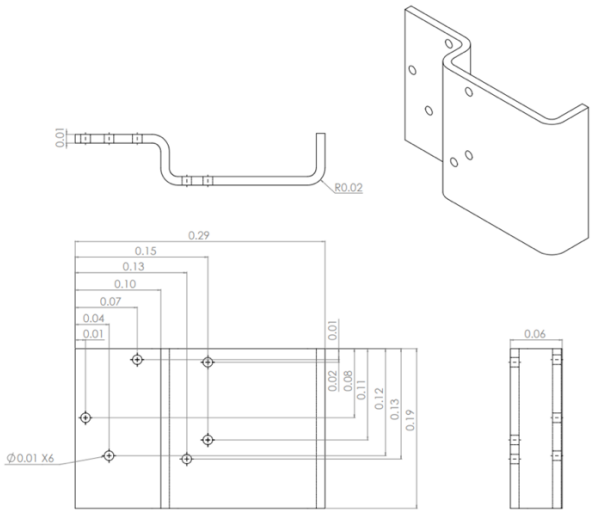

Figure 63: Metal Bracket 1 Drawing

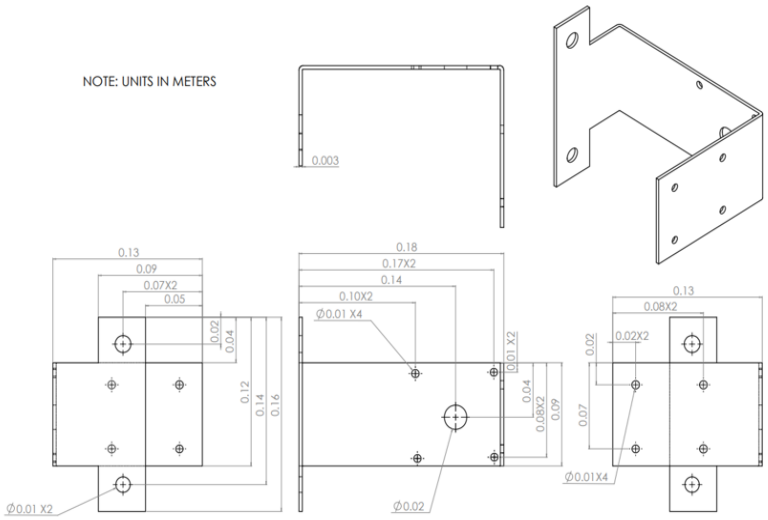

Figure 64: Metal Bracket 2 Drawing

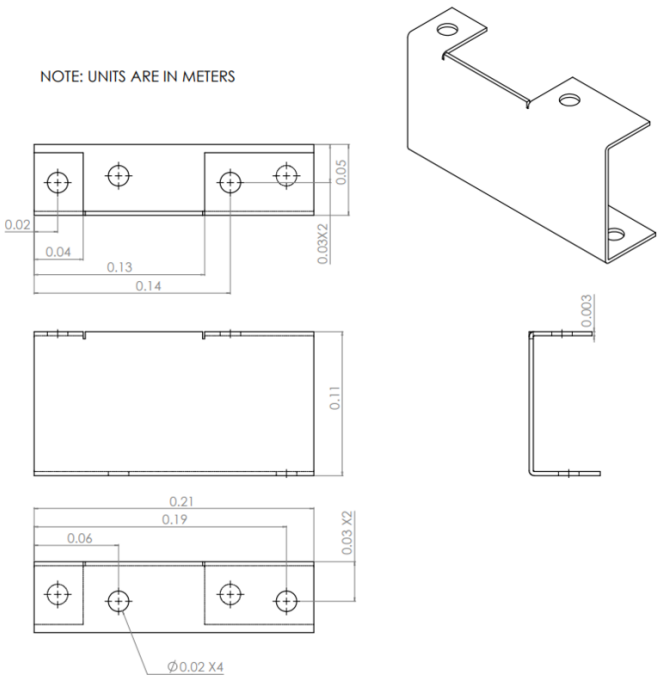

Figure 65: Metal Bracket 3 Drawing

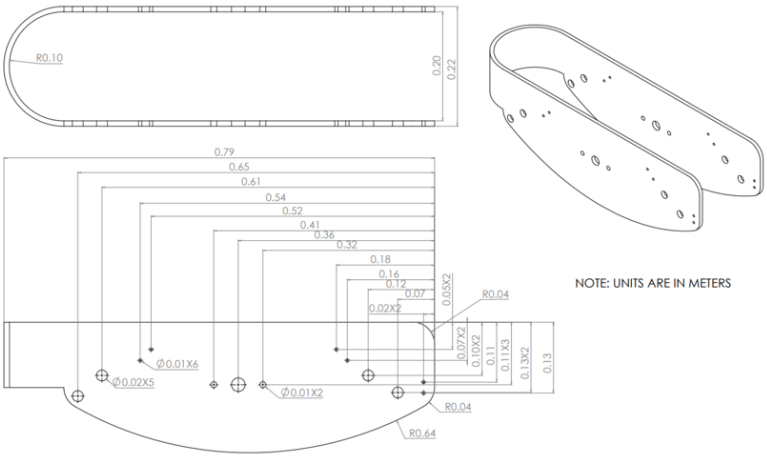

Figure 66: Metal Bracket 4 Drawing

Budget

The team performed a rough estimate of the total budget for this drivetrain. It is unclear how much any custom component will cost to manufacture, and therefore these parts were not included in the budget. These custom components include Gear 11, the wheel gear, and all shafts. Therefore, the final budget can be expected to increase substantially. Although the budget is not inclusive of the price of custom components, it provides a basis and lower limit.

Table 12: Estimated Budget For Full Drivetrain

Component	Per Item	Qty	Price
Chain	79.99	1	79.99
Gear 1	75.68	1	75.68
Gear 2	147.84	1	147.84
Gear 3	132	1	132
Gear 4	280.59	1	280.59
Gear 5	323.5	1	323.5
Gear 6	38.62	1	38.62
Gear 7	323.5	1	323.5
Gear 8	38.62	1	38.62
Sprocket 9	19.72	1	19.72
Sprocket 10	22.01	1	22.01
10mm Bearing	34.65	2	69.3
15mm Bearing	25.76	2	51.52
16mm Bearing	45.14	1	45.14
20mm Bearing	24.67	2	49.34
22.225mm Bearing	47.83	1	47.83
30mm Bearing	32.06	4	128.24
Gear 11		1	
Wheel Gear		1	
Shaft A		1	
Shaft B		1	
Shaft C		1	
Shaft D		1	
Shaft E		1	
Shaft F		1	
Total	**$**		**1,873.44**

Conclusions

The team considers this design highly viable. The design was modeled after existing electric bikes. For example, rather than solely using a motor to power the vehicle, this design is pedal assisted. Though including a pedal heavily complicated the design work, the team felt a pedal was necessary to make this device useable. It is also rated for average mountain bike speeds, pedaling speeds, and the general stresses one can expect to experience while mountain biking. Additionally, creating a mountain bike rather than a commuter bike makes this device more specific but more desired. The E-Mountain Bike market size is expected to nearly double in size over the next five years, meaning that there is a substantial demand for our niche design. All components are also expected to withstand substantially more stress than calculations require, making this design robust and long-lasting.

One advantage of this design, as mentioned, is that movement is pedal assisted rather than solely powered by a motor. This will in turn put less stress on the motor and increase the useable life of the motor. Additionally, for those experienced in riding bikes, having a pedal will feel more natural. If one were to ride a bike without a pedal, there may be a necessary learning curve to properly balance and ride the bike. Another advantage of this design is that the drivetrain is highly compact. There is substantial gear reduction undergone across the drivetrain with 9 gears, two sprockets, and 6 shafts. The team prioritized a compact and efficiently spaced design to minimize space taken up by drivetrain components.

A disadvantage of this design is the cost of the device. While the biking industry becomes increasingly expensive as specifications increase, this is still a costly device. Some aspects that increase the cost of this overall design are the requirement to custom make most shafts and one gear, and the fact that only one bike is being developed. Manufacturability of the device should

be taken into consideration to lower the cost. For example, building multiple bikes at once allows the team to buy components at bulk rather than retail pricing.

Another disadvantage of this device is that it is built around the average biking speed of 13 MPH. While this likely accounts for a majority of mountain bikers, it may not be properly rated for an elite or above average biker.

If given more time and resources, there are multiple additions the team would have liked to make to this design. Firstly, this bike is built for one size only. In the bike industry, this is not the case as every bike comes in multiple sizes to account for various heights. If given more time, the team would design this device in up to four sizes (small, medium, large, and extra- large). After undergoing the initial technology design process, it is likely that adjusting for sizes would be a much quicker endeavor.

With more time it would be useful to have a multiple speed bike. The current design only accounts for one speed whereas most bikes today have 7 to 21 speeds.

Additionally, the team would have liked to compare different motors. As most of the bike power comes from the motor, it could be beneficial to compare different motors for weight, output speed, etc.

Lastly, it would have been beneficial to build all or some of this design physically. There was an extensive learning curve and problems pointed out when transferring the design from paper to CAD. There were many flaws in the design that were not apparent until a computer model had been made. Making this device physically would only help point out additional concerns and areas for improvement in the design.

Lessons Learned

Lessons learned regarding mechanical design are that disparities may emerge between theoretical and experimental results, and that design is an iterative process. Frequently, the team created theoretical designs on paper that differed from the physical result. For example, the spacing of shafts was determined based on velocity ratios between each gear. However, when sourcing gears, there were not gears that matched our exact sizes, and the team had to rework the design based on available components.

There were also countless unknowns that made this design process highly iterative. For example, calculating bearing forces was contingent on the component spacing along a shaft. These resultant forces determined which bearings would be used. The exact spacing, though, couldn't be known until all components were picked and assembled in CAD to avoid interferences. This led to rounds of: picking bearings based on estimates, optimizing spacing in SolidWorks, and recalculating forces to ensure the bearings could withstand all required forces.

When selecting machine elements, one is often limited to available components on the market. At times there were not perfect sizes for all requirements, but the team had to build the design around existing components.

The importance of project management and wholistic scheduling became evident in this assignment. With such a large task, steps needed to be laid out in advance. Occasionally, team members inadvertently worked on the same task. A detailed schedule as well as open communication and progress checks between team members is crucial to efficient teamwork.

Lastly, mechanical design combines multiple disciplines. This project involved knowledge from multiple classes and topics. Design requires seamlessly integrating ideas across a wide variety of subjects rather than solely relying on one.

References

(1) "1045 AISI (USA) ." *Metal Data*, www.metaldata.info/reports/AISI1045.pdf. Accessed 11 Dec. 2023.

(2) "All About 3003 Aluminum (Properties, Strength and Uses)." *Thomasnet® - Product Sourcing and Supplier Discovery Platform - Find North American Manufacturers, Suppliers and Industrial Companies*, www.thomasnet.com/articles/metals-metal-products/3003-aluminum/#:~:text=The%20tensile%20yield%20strength%20for,aluminum%20a%20moderately%20strong%20material. Accessed 11 Dec. 2023.

(3) Alqahtani, Abdullah, et al. Bicycle Front Drivetrain, 17 May 2016, milan-stojanovic.com/pdf/fea-report.pdf.

(4) Baker, Antonnette. "Bicycle Weight Limit (How Much Can It Hold?)." *Bike A Ton*, 9 Feb. 2023, bikeaton.com/expert-tips/bicycle-weight-limit/#:~:text=Most%20bicycles%20are%20designed%20to%20carry%20up%20to,out%20the%20exact%20weight%20limit%20of%20your%20bike.

(5) "Bearing Selection, Load & Life." *American Roller Bearing Company*, www.amroll.com/bearing-selection-load-life.html. Accessed 11 Dec. 2023.

(6) "Cam Follower - CF-AB Series." *MISUMI*, us.misumi-ec.com/vona2/detail/221005242985/?curSearch=%7B%22field%22%3A%22%40search%22%2C%22seriesCode%22%3A%22221005242985%22%2C%22innerCode%22%3A%22%22%2C%22sort%22%3A1%2C%22specSortFlag%22%3A0%2C%22allSpecFlag%22%3A0%2C%22page%22%3A1%2C%22pageSize%22%3A%2260%22%7D&Tab=catalog. Accessed 22 Nov. 2023.

(7) Canyon. (2023, March 17). 27.5 vs 29 mountain bike: Which wheel size is best. 27.5 vs 29 mountain bike: which wheel size is best | CANYON US. https://www.canyon.com/en-us/blog-content/mountain-bike-news/27-5-vs-29-inch-mountain-bike-wheels/b17032023-2.html#bullet2-link

(8) Dey, Anup Kumar. "Factor of Safety: Definition, Equation, Examples." What Is Piping, 24 Sept. 2023, whatispiping.com/factor-of-safety/.

(9) Einstein, Halford, Weiskind, Zwayer. "Report 1 (FOS, Train VR, Bearing Location)." 3 Nov 2023.

(10) Einstein, Halford, Weiskind, Zwayer. "Report 2 (Conceptual Drawings and Design Layout)." 28 Nov 2023.

(11) "Fixed-Bore Roller Chain Sprockets." *Fixed Bore Sprockets - Roller Chain Sprockets - Grainger Industrial Supply*, www.grainger.com/category/power-transmission/roller-chains-sprockets/roller-chain-sprockets-idlers/fixed-bore-roller-chain-sprockets?categoryIndex=1. Accessed 11 Dec. 2023.

(12) Fromm, Derek, et al. "Final Design Report for Human Powered Vehicle Drivetrain Project." DigitalCommons@CalPoly, 31 May 2019, digitalcommons.calpoly.edu/mesp/489/.

(13) "General Duty plus #40 Roller Chain." *Www.Usarollerchain.Com*, www.usarollerchain.com/40-Roller-Chain-p/gdp-40-10ft.htm. Accessed 11 Dec. 2023.

(14) Gormley, Claire. "Does Crank Length Really Matter for Mountain Biking?" *Red Bull*, Red Bull, 25 Jan. 2022, www.redbull.com/gb-en/how-long-should-mtb-cranks-be.

(15) Gupta, Rajeev & Rao, G. (2017). Analysis of Mountain Bike Frame By F.E.M. 10.9790/1684-1302018994.

(16) Hurley, Sean. "Cycling Cadence: What Is It, What's Most Efficient, and Cadence Drills to Make You Faster - Trainerroad Blog." *TrainerRoad Blog Cycling Cadence What Is It Whats Most Efficient and Cadence Drills To Make You Faster Comments*, 13 Oct. 2021, www.trainerroad.com/blog/whats-the-most-efficient-cycling-cadence-and-how-cadence-drills-can-make-you-faster/#:~:text=What%20is%20a%20Good%20Cadence,%2C%20around%2060%2D85%20rpm.

(17) "Linear Ball Bearings." *MISUMI*, us.misumi-ec.com/vona2/mech/M0100000000/M0104000000/. Accessed 11 Dec. 2023.

(18) "Mountain Biking." Mountain Biking - Active & Safe, Active and Safe, activesafe.ca/mountain-biking/. Accessed 23 Oct. 2023.

(19) "Mounted Bearings and Housings." *SKF*, www.skf.com/us/products/mounted-bearings. Accessed 11 Dec. 2023.

(20) Norman, Paul. "Bicycle Chains Explained: Everything You Need to Know." *BikeRadar*, 30 Aug. 2022, www.bikeradar.com/advice/buyers-guides/bicycle-chains/.

(21) "Pillow Block Ball Bearings." *Grainger Industrial Supply*, www.grainger.com/category/power-transmission/bearings/rolling-element-bearings/mounted-rolling-element-bearings/pillow-block-bearings/pillow-block-ball-bearings. Accessed 11 Dec. 2023.

(22) "Pillow Block Bearings." *Maedler North America*, maedlernorthamerica.com/product-category/bearings-bushes-ball-transfer-units/pillow-block-bearings/. Accessed 11 Dec. 2023.

(23) "Pressure Angle." *KHK Gears*, khkgears.net/new/gear_knowledge/introduction_to_gears/pressure_angle.html#:~:text=The%20most%20common%20pressure%20angle%20is%2020%C2%B0.%20Formerly%2C,a%20pressure%20angle%20of%2014.5%C2%B0%20was%20also%20used. Accessed 11 Dec. 2023.

(24) Safety Culture. "Factor of Safety: Ratio for Safety in Design and Use." Safety Culture, 26 June 2023, safetyculture.com/topics/factor-of-safety/.

(25) "SCM415 Steel: 15CrMo." *OTAI Special Steel*, 26 July 2018, www.otaisteel.com/products/quenched-and-tempered-alloy-steels/jis-scm415/.

(26) "Spur Gears." *KHK Gear Manufacturer*, khkgears.net/new/spur_gears.html. Accessed 11 Dec. 2023.

(27) Stott, Seb. "Nerding out: Why a Lower Shock Position Doesn't Make a Bike More Stable." *Pinkbike*, 17 May 2022, www.pinkbike.com/news/nerding-out-why-a-lower-shock-position-doesnt-make-a-bike-more-stable.html#:~:text=Just%20like%20increasing%20the%20wheelbase,avoid%20going%20over%20the%20bars.

(28) Stott, Seb. "Nerding out: Why You Shouldn't Worry Too Much about Weight." *Pinkbike*, 20 Oct. 2021, www.pinkbike.com/news/why-you-shouldnt-worry-about-weight-much.html.

(29) Wright, Jesse. “How Fast Does a Mountain Bike Go?: Pedal Chile.” Pedal Chile, Pedal Chile, 9 May 2021, pedalchile.com/blog/mtb-speed#:~:text=Uphill%20sections%20average%20%E2%89%88%208,12%20mph%20(19%20kph).&text=%EF%BB%BFThe%20average%20speed%20is,during%20downhill%20mountain%20bike%20riding.

(30) Zinn, Lennard. “Technical FAQ: Weight Distribution, Compatibility, and More.” *Velo*, 1 June 2023, velo.outsideonline.com/road/road-racing/technical-faq-weight-distribution-compatibility/.